1.0

4.5
5.0
5.5

2.8   2.5

3.2   2.2

3.6

4.0   2.0

1.1

1.8

1.25   1.4   1.6

MICROCOPY RESOLUTION TEST CHART
NATIONAL BUREAU OF STANDARDS-1963-A

National Research / Conseil national
Council Canada   de recherches Canada

CENTRIFUGAL BLOWER NOISE STUDIES LITERATURE SURVEY AND NOISE MEASUREMENTS

BY

G. KRISHNAPPA

DIVISION OF MECHANICAL ENGINEERING

FEB 25 1977

OTTAWA

DECEMBER 1976

CENTRIFUGAL BLOWER NOISE STUDIES

LITERATURE SURVEY AND NOISE MEASUREMENTS

(6)

ETUDES DES BRUITS ASSOCIEES A L'UTILISATION DES SOUFFLEURS CENTRIFUGES

ETUDE DE LA LITTERATURE SPECIALISEE ET MESURES DES BRUITS

(11) Dec 76

(12) 56p.

(14) DME-ME-244

by/par

(10) G. Krishnappa

(18) NRC
(19) 15679

244 050
bpg

E.H. Dudgeon, Head/Chef
Engine Laboratory/
Laboratoire des moteurs

D.C. MacPhail
Director/Directeur

SUMMARY

A review of the existing literature on the subject of centrifugal fan and blower noise studies is presented in this report to establish further areas of research needed to aid in the development of a quiet blower. Noise measurements on a wide variety of blowers used in the laboratory, ranging from 1/3 to 700 horsepower are described, with the object of identifying important frequency components from various types of blowers.

The blade passing frequency tone and its harmonics are shown to be produced by the interaction of the flow issuing from the blade exit with the cut off edge formed by the junction of the blower casing and its exhaust duct. The clearance distance between the cut off edge and the impeller blade tip is recognized to be an important parameter in reducing these tones. The random noise is generated by the unsteady flow processes within the impeller. The empirical equations developed to predict the sound power generated have been shown to give a rough estimation of the broadband noise but cannot estimate the tones with adequate accuracy. Attempts have been made to establish fan noise laws based on similarity principles to predict the noise from a group of similar machines based on detailed measurements on a single model fan. The influence of Mach number, Reynolds number, Strouhal number and flow coefficients is discussed.

The blower casing and ducted environment are shown to exert a powerful influence on noise characteristics. The effects of the casing and ducted environment on blower noise have been discussed on the basis of the theory of black boxes as used in communication engineering, and the lumped impedance model. While these methods help the understanding of the acoustical behaviour of the fan system, they fail to describe adequately the effects of the casing and ducted environment, especially at high frequencies. Acoustical resonance effects in small blower casings are discussed.

Among the various blowers tested, the prominent noise component appeared to be the tone at the blade passing frequency. There were two exceptions, in that the noise characteristic of a large 700 horsepower blower was predominantly broadband, but a small 1/3 horsepower blower indicated the absence of the blade passing frequency tones and the presence of a tone due to the struts supporting the blades.

(français verso)

SOMMAIRE

Nous présentons une critique de la documentation qui existe au sujet des études de bruit des ventilateurs rotatifs et des souffleurs centrifuges. Le but de ce rapport est d'établir les domaines de recherche nécessaires au développement d'un ventilateur centrifuge à bruit réduit.

Nous rapportons aussi les résultats des mesures de bruit d'une variété de ventilateurs soufflants qui se trouve dans ce laboratoire, de puissance à la portée de 1/3 cv à 700 cv. Le but de cette recherche était d'identifier les fréquences importantes qui sont produites par des types variés de ventilateurs.

La littérature suggère que la fréquence du passage des ailes et ses harmoniques se produisent par l'action du débit d'une aile en passant par la jointure du chassis du ventilateur et la conduite pour la sortie de l'air.

Le bruit de fond est produit par le débit irrégulier dans la région de la roue. L'enveloppe du ventilateur et l'environnement de la conduite déploient une influence puissante sur la bruit caractéristique.

Les résultats des essais montrent que la composante saillante du bruit est le ton à la fréquence des ailes passantes.

CONTENTS

ILLUSTRATIONS

ILLUSTRATIONS (Cont'd)

ILLUSTRATIONS (Cont'd)

SYMBOLS

Symbol	Definition
A, A_1, A_2	amplifications and quality factors
a_0	speed of sound
B	number of impeller blades
C_A	acoustical compliance
c_{m_2}	meridonal velocity
D, D_1, D_2	diameter of impellers
F	function of Strouhal number
f	frequency

SYMBOLS (Cont'd)

Symbol	Definition
f_0	resonance frequency
G	function of Helmholtz number
g	acceleration due to gravity
H	head
He	Helmholtz number
HP	horsepower
I_0, I_1, I_2	current
i_1, i_2	current
i_{10}	current source quantity
k	wave number
L	length of duct
L_i	length of inlet duct
L_0	length of outlet duct
l_c	length of constriction
l_e	correction length
M	Mach number
M_A	combined inertance
M_{A_1}	inlet inertance
M_{A_2}	outlet inertance
N	rpm
n_s	specific speed
p_S	static pressure
p_T	total pressure
$\tilde{p}$	mean sound pressure

SYMBOLS (Cont'd)

Symbol	Definition
p_1, p_2	sound pressure
p_{10}	pressure source quantity
Q	discharge flow
q_{10}	velocity source quantity
R	Reynolds number
R_A	acoustical resistance
$R_1 - R_5$	complex reflection factor
$r_1, r_2, \ldots$	radius
S	Strouhal number
S_t	Normalized Strouhal number for blade passing frequency tones
S_i	inlet area
S_o	outlet area
$S_1, S_2, \ldots$	area
u_2, u_{21}, u_{22}	tip speed of the impeller
V	volume of the casing
v_1, v_2	voltage
v_{10}	voltage source quantity
V_R	volume of the rotor passages
x	distance along the duct
Y_R	admittance function
Y_e	load admittance
Z_e	load impedance
$Y_1, Y_2, \ldots$	admittance
$Z_1, Z_2, \ldots$	impedance

SYMBOLS (Cont'd)

Symbol	Definition
α	Mach number exponent
β	Reynolds number exponent
γ	isentropic exponent of working fluid
η	efficiency
λ	wavelength
ν	kinematic viscosity
ρ	density of air
ρ_o	density of the ambient air
ϕ	flow coefficient
ψ	pressure coefficient
ω	angular frequency
ω_o	angular frequency at resonance

CENTRIFUGAL BLOWER NOISE STUDIES
LITERATURE SURVEY AND NOISE MEASUREMENTS

1.0 INTRODUCTION

Centrifugal blowers and fans are used in a wide range of applications, from small fractional horsepower fans in household heating and ventilating systems to large blowers to pump air in industrial processes operating at several hundred horsepower. Some of these blowers and fans are relatively quiet, but a majority of them are very noisy. The noise produced by each type of blower depends not only upon its capacity to pump air but also on its design, fabrication and the ducted environment into which the machine is compelled to operate. Due to growing public awareness, there is a recurring requirement for quiet fans and blowers and it is becoming common to include the acoustic performance of the fan in its specification.

The noise from these machines could be controlled by fitting silencers to the air moving systems, since these silencers are commercially available in various sizes and capacities. This would undoubtedly add to the cost and bulk of the system. Therefore, there is a clear need for developing quiet blowers by controlling the noise generated at the source itself. This should be accomplished by suitably designing the various elements of the fan contributing to the generation of noise without degrading the performance.

The flow processes inside a centrifugal blower are very complex and as a result, the design and fabrication of these machines vary widely among manufacturers. The earlier work on noise aimed at developing empirical equations for a similar set of machines relating the noise output to the various operating parameters such as flow, velocity, pressure rise, speed, horsepower, etc. While there have been some useful papers published recently on the fundamental mechanism of noise generation, propagation and radiation inside the impeller and its ducted environment, the number of papers is very limited. There also appears to be a need for improved techniques for ducted fan noise measurements, as the existing standards need refinement.

The Engine Laboratory of the National Research Council has embarked on a research programme to identify and suggest means of controlling the noise in centrifugal blowers and fans. The laboratory has been actively involved for several years in examining the flow distribution in a centrifugal compressor impeller in order to develop an understanding of the complicated flow processes. The expertise available in the laboratory on the aerodynamics of blowers is expected to aid in the research programme in understanding the noise producing mechanism inside the blowers. The initial objective of the programme clearly is to define the areas where further research is needed. Later work will include testing of a series of model fans by modifying several fan design parameters identified as contributors to noise generation and propagation.

In this report the existing literature on this subject is reviewed to establish further areas of research. The results of a noise survey conducted on a wide variety of blowers from 1/3 to 700 horsepower existing in the laboratory are presented. The noise measurements were made on the various blowers with the object of identifying the important frequency components and relating them to the various elements of the duct blower system.

2.0 CENTRIFUGAL BLOWERS

A centrifugal blower or fan consists essentially of two parts as shown in Figure 1: an impeller and a casing enclosing the impeller. Energy is transferred to the air by the rotating impeller. The casing guides the gas into the impeller and leads it away at a higher pressure. Various types of centrifugal blowers and fans are dictated by the operating requirements and each class differs in its design and manufacture. Impellers are often classified according to the blade angle at the outlet, as shown in Figure 2. Forward curved bladed impellers where the outlet blade angle $\beta_2 > 90°$ have a narrow range

of stable operation. Backward curved blades with $\beta_2 < 90°$ have a wider range of operation with higher efficiencies. Most industrial blowers have straight radial blades, ($\beta_2 = 90°$) as these are relatively easy to manufacture of fabricated steel plate. Low efficiency in fans is usually the result of sacrificing smooth flow for simplicity of manufacture, small size and weight, and low cost.

After the air leaves the impeller, the velocity is reduced and partially converted into pressure by diffusion. A vaneless diffuser is used to reduce the impeller discharge velocity before it is collected in a volute casing. The "vaneless diffuser" usually consists of two parallel plates where, ideally, the air travels through the diffuser at the same angle as that at which it leaves the impeller, and the velocity is reduced in the inverse ratio of the inlet and outlet diameters. Figure 3 shows a vaned diffuser in which the direction and velocity are controlled by the vanes, resulting in a more efficient conversion of velocity into pressure. These diffusers are normally used in high pressure and more sophisticated blowers, usually in aircraft applications. In a volute casing, air from the impeller is collected at constant velocity in a volute channel and all diffusion is accomplished by a diffuser outside the casing.

3.0 AERODYNAMIC NOISE SOURCES

Noise generated inside a centrifugal blower is of aerodynamic origin. The mechanism of noise generation can be explained on the basis of aerodynamic noise theory. It is generated within the casing by the action of the impeller blades and propagates through the inlet and exhaust ducts. The noise spectrum from a centrifugal blower generally consists of tones at the blade passing frequency and its harmonics superimposed on broadband noise. Figure 4 shows the noise spectrum measured inside the exhaust duct of a 15 horsepower blower in one-third octave bandwidths. In this spectrum only the fundamental of the blade passing frequency tones is prominent, and high levels of broadband noise are present at frequencies below 1000 Hz.

The theory of aerodynamic noise has shown that fluid flow in the presence of solid boundaries generates dipole sound. Unsteady flow on solid boundaries would cause fluctuating forces acting on the solid surface which could generate both discrete tones and broadband noise. Discrete tones are generated by periodic forces, while random forces acting on the solid boundary produce broadband noise.

The flow in a centrifugal impeller is very complex, as the flow confined within the blade channels changes its direction in three dimensions and strong rotations are induced into the fluid flow. The flow is further modified by boundary layer and leakage effects, and the whole of this takes place in an unstable diffusing flow regime. Flow in an impeller channel as sketched and verified by Fowler (Ref. 1) is shown in Figure 5. Even at the design point, there would be a detached flow region at the suction wall trailing edge. With reduced flow the detachment zone would increase, creating unsteadiness in the flow relative to the rotating impeller.

While the pressure field associated with rotating impeller blades can generate both discrete tones and broadband noise, the major source of the blade passing frequency tone in a blower without diffuser vanes is produced by the passing of the impeller blades past a fixed cut off. The flow issuing from the blade passages encounters the cut off edge where the fan casing and the diffuser duct meet as shown in Figure 1.

Experimental measurements by Chanaud (Ref. 2) and Embleton (Ref. 3) have established the effectiveness of this cut off edge in generating blade passing frequency tones. By placing a fixed wedge near the pheriphery of an uncased impeller, Chanaud (Ref. 2) verified that this source had the characteristics of a point dipole. Embleton (Ref. 3) has shown that by locating the cut off at the optimum distance from the tips of the blades, large reductions in the levels of the blade passing frequency tone and its harmonics may be obtained. This optimum clearance appears to vary for each harmonic for minimum noise levels as shown in Figure 6. The shape of the velocity profile varies across the width of the blade channel outlet and hence has Fourier coefficients that change with the radial distance. If the cut off is located at such a distance that any of the Fourier coefficients is zero,

the resulting output at that frequency is minimum. By sloping the cut off edge relative to the blade tips, some reductions can be expected as the excitation along the cut off edge will differ in phase (Ref. 3).

Published data on the increase in noise level due to the presence of vaneless or vaned diffusers or inlet guide vanes are lacking. As the non-uniform flow from the impeller blade passages is intercepted by a vaned diffuser, a drastic rise in the level of the blade passing frequency tone may be expected. The presence of inlet guide vanes may generate a less severe effect; however, there would be an increase in the tone levels. In fact, in axial flow fans the dominant mechanism generating blade passing frequency tones is the interaction between rotor and stator blades. The wakes shed by the rotor or stator blades are intercepted by the succeeding blade row. Because of the change in the angle of incidence of the flow at the leading edge of the blades, unsteady lift is produced. Thus, the blade row forms an array of dipole noise sources with sequential phasing depending on the wake interaction events. The spacing between the rotor and stator blades has a pronounced effect on the tone levels; an increased spacing reduces the levels. Similarly it may be desirable to have large spacings between the diffuser vanes and the impeller blades.

Broadband noise is generated within the blower due to the unsteady flow processes involved. At operating points away from the design point, the unsteadiness associated with the flow would increase, enlarging the detachment zone on the trailing side of the rotor vane. Broadband noise is produced by the random and roughly periodic eddies thus formed within the flow.

4.0 EMPIRICAL EQUATIONS FOR NOISE ESTIMATION

Early work on centrifugal fan noise was concerned mainly with formulating empirical equations for predicting the total sound power levels and octave band frequency spectra in terms of the operating parameters of the fan. Based on tests on fourteen dissimilar commercial fans, Beranek, Kamperman and Allen (Ref. 4) established the following equations for the total sound power level within ± 4dB in terms of the operating parameters.

$$\begin{aligned}
SWL &= 90 + 10 \log HP + 10 \log p_S \\
&= 55 + 10 \log Q + 20 \log p_S \\
&= 125 + 20 \log HP - 10 \log Q
\end{aligned} \qquad (4.1)$$

where

SWL is the overall sound power level in dB relative to 10^{-12} watt

Q is the discharge flow in cfm

p_S is the static pressure in inches of water.

Thus by knowing any two of the operating parameters: horsepower, pressure and discharge flow of the fan, sound power level can be estimated approximately. The spectral shape of the noise may be calculated for backward or forward curved blades by substracting 7dB from the total sound power levels for the 125 Hz octave band and subtracting 5dB per octave band from there onwards. The noise spectrum for large backward curved blades is predicted by shifting the spectrum to the right until the value shown for the first octave band lies in the octave band containing the blade passing frequency. Above the blade passing frequency the level in each octave band is estimated to decrease by 5dB per octave. This prediction method may not apply to fans with radial blades. Baade (Ref. 5) has shown in Figure 7 that the above prediction method gave good agreement within ± 4dB on a wide variety of commercial ventilating fans of similar size excluding those with backward curved blades. The agreement is satisfactory especially in the lower frequency range. In the case of backward curved blades, Figure 8 from Reference 5 shows that while broadband noise can be predicted within ± 2dB, the blade passing frequency tone cannot be estimated with adequate accuracy because of the difficulty of measuring the blade passing frequency tone within the existing standards.

While no aerodynamic or mechanical details of the fan elements were taken into consideration in formulating the above prediction procedure, it was meant to be used as a rough guide for specifying commercial silencers after a fan had been selected for a ventilating system.

5.0 FAN NOISE LAWS

5.1 Fan Performance Laws

The application of similarity principles to the aerodynamic performance of fans is well established. The performance law is valid for a family of geometrically similar machines relating the non-dimensional parameters. The advantage of this principle is that a series of dimensional curves for a group of machines collapses into a single curve on non-dimensional representation. These curves enable experiments carried out on a small scale model to be applied to the design of a large machine.

For centrifugal blowers of similar types the performance curves (in the incompressible flow regime) are represented by one single curve of pressure or head coefficient as a function of flow or capacity coefficient.

That is:

$$\psi = f(\phi) \tag{5.1}$$

The pressure coefficient

$$\psi = \frac{p_T \text{ or } p_S}{\rho u^2_2} \tag{5.2}$$

and the flow coefficient

$$\phi = \frac{c_{m2}}{u_2} \tag{5.3}$$

where

p_T or p_S is the total or static pressure rise

ρ is the density of air

u_2 is the tip speed of the impeller in ft./sec.

c_{m2} is the meridonal velocity at the discharge side of the impeller.

Similarly, the efficiency of a particular design of impeller is plotted as a function of flow coefficient. Generally the flow coefficient is used as an independent parameter in the performance analysis of the blower. It may be noted that the same performance curve is valid for all impeller speeds. However, if the viscosity of the air is considered, another independent parameter, the Reynolds number R must be considered, which may be of the form $\frac{u_2 D}{\nu}$, where D is the diameter of the impeller and ν is the kinematic viscosity. Blower performance curves are known to vary slightly over a wide range of Reynolds numbers.

For a given design, an optimum efficiency point would exist for a certain speed and flow combination. In the incompressible flow range, fans are classified according to a number known as the specific speed given by the formula

$$n_s = \frac{Q^{1/2}N}{H^{3/4}} \tag{5.4}$$

where H is the head and N is the rotational speed of the fan. The point of maximum efficiency of similar machines has the same specific speed irrespective of fan size or speed and therefore this number is closely associated with the impeller geometry.

5.2 Noise Similarity Laws

Various attempts have been made to establish fan noise laws. With these laws the sound produced by a whole group of similar machines could be predicted from detailed measurements on only one fan belonging to the group. Madison (Ref. 6) was the earliest to derive an expression relating the diameter and tip speed to the total sound power level:

$$SWL \propto D^2 u_2^5 \tag{5.5}$$

The derivation of this expression is based on the assumption that the sound power level was proportional to the volume flow and to the square of the static pressure difference. Chanaud (Ref. 2), using the aerodynamic noise theory, derived the following expression for the dipole sound generated within an impeller

$$SWL \propto \rho u_2^3 D^2 M^3 \propto \rho N^6 D^8 \tag{5.6}$$

where M is the tip Mach number.

Experiments performed by various workers have shown that, depending on the type of fan or blower and the method of measurement, the exponent of speed will be between four and six, and the diameter exponent between six and eight. The values of the tip speed exponent found by various workers are tabulated in Reference 7. Large experimental deviations show additional dependence of sound levels on other fan operating parameters. Maling (Ref. 8), using dimensional analysis, showed that generated sound levels also depended on

Mach number $\quad M = \dfrac{u_2}{a_0}$

Reynolds number $\quad R = \dfrac{u_2 D}{\nu}$

Strouhal number $\quad S = \dfrac{fD}{u_2}$

Flow coefficient $\quad \phi = \dfrac{c_{m2}}{u_2}$

where f is the frequency.

Experiments by Chanaud (Ref. 2) on a free running uncased rotor showed that the overall sound power levels varied according to N^5D^7, the original fan noise law proposed by Madison (Ref. 6). There was agreement only at the lower Strouhal numbers, with large deviations at higher Strouhal numbers. However, when a wedge was placed close to the periphery of an uncased impeller, the sound power levels varied according to the dipole law. While Mach number dependence is implicit in the dipole expression, Chanaud's experiments (Ref. 7) showed weak dependence on Reynolds number and flow number.

However, Deeprose and Brooks (Ref. 9) have demonstrated the influence of flow coefficient and Reynolds number in establishing the similarity relationship on a backward curved impeller with aerofoil section blades. They did not consider the effect of Strouhal number in their investigations. Figures 9 to 12 show, for two specific speeds of 0.822 and 1.466, the effect of flow coefficient on performance and total acoustic power. In both cases the minimum noise occurs at the flow coefficient corresponding approximately to the best efficiency point. With the higher specific speed there is a steep rise in noise levels as stall conditions are approached, due to the severity of stall with this type of rotor. The change in noise level at the lower specific speed is more gradual as the stall was less severe. The indices for both N and D varied between the two specific speeds. However, the variation in the measured results could be accounted for by the Reynolds number dependence:

$$SWL = \rho N^6 D^8 f(R) \tag{5.7}$$

The mean index for Reynolds' number was found to be 1.24 ± 0.62.

The application of the similarity principle to the blade passing frequency tones has been demonstrated by Neise (Ref. 7). The dependence of sound on Strouhal number was considered in the investigation, which effect had not been thoroughly investigated by the earlier workers. In this analysis the general relationship among the non-dimensional parameters developed by Weidemann (Ref. 10) was adopted, giving sound pressure (which is the square root of the sound pressure level)

$$\widetilde{p} = F\left(M, R, S, \phi, \frac{x}{D}, \gamma\right) \tag{5.8}$$

where x is the measuring position along the exhaust duct and γ is the isentropic exponent of the working fluid. This formulation is similar to the parameters derived by Maling (Ref. 8) except for the additional variable of a gas constant and the measurement position. This expression, for a constant flow coefficient and for the same working fluid, was expressed as a product:

$$p = M^\alpha R^\beta F(St)G(He) \tag{5.9}$$

where the normalized Strouhal number $St = \dfrac{fD}{u_2}\dfrac{\pi}{B}$ and $He = \dfrac{D}{\lambda} \propto M \cdot St$

He is the Helmholtz number, B is the number of blades and λ is the wave length. The normalized Strouhal number ST = 1 corresponds to the blade passing frequency and St = 2, 3, 4 . . . describe its higher harmonics. While the influence of tip speed, impeller diameter, and viscosity are described by Mach number and Reynolds number, the spectral composition of sound is described by F(St), and G(He) determines the acoustic frequency response function describing the radiation characteristics of the fan and its casing.

For overall sound pressure, identical values of α and β are assumed for all Strouhal numbers. Then

$$p \propto u_2^{\alpha+\beta}D^\beta \tag{5.10}$$

The spectral distribution function can be determined by

$$p \propto M^{\alpha} R^{\beta} F(St) \text{ when He = const.}$$

$$\text{or } p \propto u_2^{\alpha+\beta} F(St) \text{ when He = const., D = const.}$$

The acoustic frequency response function can be determined by

$$p \propto G(He) \, u_2^{\alpha+\beta} \text{ when St = const. and D = const.}$$

Two dimensionally similar fans of 140 mm and 280 mm diameter were tested by Neise (Ref. 7) to verify the similarity formulations. The distance between the impeller tip and cut off edge was maintained very small in order to excite a large number of blade passing frequency harmonics. This seems to have been necessary in the experiments to study the sound radiation at various Strouhal numbers. The measurements were carried out in exhaust ducts with anechoic terminations according to the ISO proposal TSO/TG43/SC1/WG3.

The experiments indicated a Reynolds number exponent $\beta = 0.2$ and a Mach number exponent $\alpha = 2.1$, showing a variation of sound pressure with tip speed of $u_2^{2.3}$. Figure 13 shows the overall sound pressure level as a function of tip speed, and the similarity relationship is in agreement for the two fans. The assumption that the constant Strouhal number curves exhibit the same frequency characteristics is also valid as shown in Figure 14. The acoustic frequency response function G(He) was determined from Figure 14, based on the deviation of each curve from the average $u_2^{2.3}$ dependence of sound pressure. A comparison of the results from both fans is shown in Figure 15, which indicates reasonable agreement. Similarly in Figure 16 is shown the comparison of the spectral distribution function F(St) determined from the vertical distance between the curves of constant Strouhal number in Figure 14, after correcting according to $u_2^{2.3}$ for impeller speed dependence. The blade passing frequency tones were strongly excited with decrease in tone levels with an increase in the harmonics. Again there appears to be reasonable agreement with similarity formulations.

The experimental results of Deeprose and Brooks (Ref. 9) and Neise (Ref. 7) reveal that the similarity formulations of Maling (Ref. 8) and Weidemann (Ref. 10) are valid and that the experimental data from a model fan may be scaled to dimensionally similar full size fans.

5.3 Selection of Fans for Minimum Noise

Based on similarity principles, it is possible to select a fan for minimum noise for a given pumping requirement. Assuming that the noise level for a given family of fans of similar design at a given flow coefficient depends on the tip speed and diameter of the fan, Mellin (Ref. 11) has discussed the selection of fans for minimum noise. Reynolds number and Strouhal number effects were not taken into consideration. Measurements by Deeprose and Brooks (Ref. 9) have shown that the noise output is minimum when the fan is operating at a flow coefficient corresponding to the best efficiency point. Comparing the two families of fan design shown in Figure 17, for the same operating point fan A performs at peak efficiency with lower noise levels, and fan B would do the same task at relatively lower efficiency with higher noise levels. At the flow coefficient corresponding to the peak efficiency point of fan B, fan A could operate at a higher noise level than fan B. Therefore it is essential to design a fan to perform close to the peak efficiency point at the flow coefficient corresponding to the flow requirement. The noise output at the flow coefficient for minimum noise can be used to compare one fan design with another in determining the optimum design for a particular task.

The type of fan design to give the required flow rate and pressure rise can be selected among several available design families the non-dimensional parameters, flow coefficient, and pressure coefficient of which should correspond to the peak efficiency point. Within the same family of designs based on rather simplified noise laws, the noise levels depend on the size and speed of the fan (Figs. 18 and 19) according to the relation

$$SWL \propto u_2^x D^2 \tag{5.11}$$

where the value of the exponent x usually lies between four and six. By substituting the fan performance parameters into Equation (5.11), the speed and diameter of the fan for performing a given pumping task at minimum noise levels can be determined. A detailed analysis of this procedure is given in Reference 11.

6.0 EFFECT OF CASING, HOUSING GEOMETRY, AND DUCT ENVIRONMENT

While the noise produced by fans and blowers is generated by sources which are aerodynamic in origin, the characteristics of the noise cannot be described by the aerodynamic parameters alone because the casing and the duct system exert a powerful influence on the noise characteristics. The geometry of the casing and ducting may be expected to affect the source characteristics by presenting considerable back reaction to the generating sources, as the generated noise depends on the nature of the impedance presented to the sources. The rotor casing, outlet casing, neck, diffuser duct, inlet and exhaust ducts all present different input and output impedances, depending on their geometry. Figure 20 shows the effect of the housing on the noise generated by a small forward curved impeller. These spectra indicate that the addition of the housing has increased the sound power level over most of its frequency range with the predominant increase at 400 Hz corresponding to the Helmholtz resonance frequency.

6.1 Treatment of Fans as Black Boxes

Cremer (Ref. 12), by extending the black box theory approach used by communication engineers, has treated the problems of fan noise relating to the casing and ducted environment provided to a fan system. A brief review of the theory of black boxes as applied to communication networks and their analogue representations of the problems of fan noise is given here. Figure 21 shows the one port and two port system passive black boxes. If there are no voltage sources inside the black box, it is termed a passive black box, and the presence of voltage sources inside the black box makes it an active one. A passive one port black box may be characterized by an impedance

$$Z_1 = \frac{v_1}{i_1} \tag{6.1}$$

Where v is the voltage and i is the current.

If the black box has two pairs of poles the two voltages can be expressed as functions of two currents, that is

$$v_1 = Z_{11}i_1 + Z_{12}i_2$$

$$v_2 = Z_{21}i_1 + Z_{22}i_2 \tag{6.2}$$

or alternatively the two currents as functions of two voltages, and also the two quantities at the input side may be expressed as those at the output.

If the voltage v_2 or current i_2 is a given quantity on one side of the two port box, this can be included inside the box itself and then the box becomes an active one port box as shown in Figure 22(a). This may be represented as a voltage source, as shown in Figure 22(b), which is in series with an internal impedance Z_1, or as a current source, in Figure 22(c), which is in parallel with an internal admittance Y_1. Z_1 and Y_1 may be determined from the open and short circuited impedances of the passive two port box. The voltage source quantity v_{10} or the current source quantity i_{10} in Figure 22 can be calculated from the voltage v_2 or the current i_2 and the measured impedance quantities. The current i_1 or the voltage v_1 may be calculated for any given internal and load impedances or admittances by the following equations:

$$i_1 = \frac{v_{10}}{Z_1 + Z_e}$$

(6.3)

$$v_1 = \frac{i_{10}}{Y_1 + Y_e}$$

where Z_e and Y_e are the load impedance and admittance respectively.

Analogue representations of a fan for one port and two port systems are shown in Figure 23. Sound pressure p and volume velocity q correspond to the voltage v and current i respectively, and the equations for the fan system are given by

$$p_1 = p_{10} - Z_1 q$$

(6.4)

$$q_1 = q_{10} - Y_1 p_1$$

Where an impedance $Z = \dfrac{p}{q}$, an admittance $Y = q/p$, and p_{10} and q_{10} are pressure and velocity source quantities similar to v_{10} and i_{10}.

The derivations of similar equations for two port active systems are given by Cremer (Ref. 12). The above equations are useful for sinosoidal components like the blade passing frequency tones; for random noise a measure of correlation coefficient and cross power spectral density are required.

It may appear that the black box approach is rather academic and may not be suitable for attacking practical problems. Wollherr (Ref. 13) has demonstrated the practical application of the theory in understanding the acoustical behaviour of a fan system. It is not as easy to achieve open poles, which makes q = 0, and short circuited poles, with p = 0, in acoustical systems as in electrical systems. These conditions Wollherr (Ref. 13) approximated by having the length of the duct

$$L = \frac{n\lambda}{2} \ (n = 1, 2, \ldots .) \text{ for } p = 0$$

and

$$L = L(2n + 1)\frac{\lambda}{4} \ (n = 1, 2, \ldots .) \text{ for } q = 0$$

Figure 24 shows the schematic test arrangements for determining the two port parameters of centrifugal fans. By measuring the complex impedance quantities by pressure ratios and pressure velocity ratios, Wollherr (Ref. 13) evaluated the internal impedances Z_1, and Z_2 for the inlet and outlet of a ducted centrifugal fan. These impedances correspond to the internal impedance in Equation (6.3) with one side having a constant duct length.

Wollherr (Ref. 13) also demonstrated that the blade passing frequency tone was generated by the passing of the blades past the cut off edge forming dipole sources. An artificial dipole source was placed at the cut off edge and the difference between the sound radiated through the inlet and outlet ducts was measured at the blade passing frequency of an experimental fan. Figure 25 shows reasonably good agreement in the peak sound level difference between an experimental fan and an artificial dipole source.

It is possible to determine the q_{10} value in the equation $q_1 = q_{10} - Y_1 p_1$ which characterizes the source value independent of the external load (ducting) for the one port active system. Figure 26 shows the test arrangement with a permanent inlet; the admittance Y_1 of the fan system can be determined by the impedance tube method. By measuring the sound pressure level p_1 for the blade passing frequency tone and $\overline{p_1}^2$ for the random noise, the values of $|\overline{q_{10}}|^2$ can be estimated. Figure 27 shows the results of Wollherr (Ref. 13), which characterize the fan as a source independent of the external load, showing also the variation with velocity in the duct system.

6.2 Acoustical Resonances in Casings

In blowers used in room air conditioners, Moreland (Ref. 14) identified enhancement in noise levels at frequencies corresponding to the resonance frequencies of the housings. For wave lengths greater than the largest housing dimensions, the lowest resonance frequency corresponds to the Helmholtz resonance frequency, which can be calculated by the lumped parameter analogy. Because of the complicated geometry of the housing, it is difficult to calculate the higher resonance frequencies which correspond to the eigen frequencies of the housing.

Figure 28 shows acoustical models of single and double inlet blowers and their electrical analogues.

Combined inertance or acoustical mass is given by the electrical analogue

$$M_A = \frac{M_{A1} M_{A2}}{M_{A1} + M_{A2}} \qquad \text{for single inlet}$$

$$(6.5)$$

$$M_A = \frac{M_{A1} M_{A2}}{M_{A1} + 2M_{A2}} \qquad \text{for double inlet}$$

where M_{A1} and M_{A2} are the acoustical inertances of the inlet and outlet respectively. The ratio of current in the resistive branch I_2 to the source current I_0 in the analogues is

$$\frac{I_2}{I_0} = \frac{- j/\omega C_A}{R_A + j \left(\omega M_A - \dfrac{1}{\omega C_A} \right)} \qquad (6.6)$$

At resonance, $\quad \omega_o M_A = \dfrac{1}{\omega_o M_A} \qquad$ (reactance is zero)

The sound power radiated at resonance is proportional to the current I_2 in the resistive branch. The amplification at resonance, defined as the quality factor, is

$$A = \frac{\omega_o M_A}{R_A}$$

For an unflanged opening the resonance frequency f_o can be calculated in terms of the blower housing geometry by

$$f_o = \frac{a_o}{2\pi} \left[\frac{L_i S_o + L_o S_i}{L_i L_o V} \right]^{\frac{1}{2}} \qquad \text{single inlet} \qquad (6.7)$$

and
$$f_o = \frac{a_o}{2\pi} \left[\frac{L_i S_o + 2L_o S_i}{L_i L_o V} \right]^{\frac{1}{2}} \qquad \text{double inlet} \qquad (6.8)$$

L_i and L_o are inlet or outlet lengths including the corrections

S_i and S_o are inlet or outlet opening areas

V is the volume of the casing

Similarly, quality factors for single inlet and double inlet blowers are

$$A_1 = 4\pi \left[V \left(\frac{L_i L_o}{L_i S_o + L_o S_i} \right)^3 \right]^{\frac{1}{2}} \qquad \text{single inlet} \qquad (6.9)$$

$$A_2 = 4\pi \left[V \left(\frac{L_i L_o}{L_i S_o + 2L_o S_i} \right)^3 \right]^{\frac{1}{2}} \qquad \text{double inlet} \qquad (6.10)$$

The above equations indicate two important differences between single and double inlet blower housings. Single inlet blowers have lower resonance frequencies than their double inlet counterparts, and the resonance amplification for a double inlet blower is less than that of a single inlet blower.

Moreland (Ref. 14) experimentally demonstrated the existence of peaks at the Helmholtz resonance frequency for small blowers with forward curved blades. The sound power levels radiated by a single inlet 7-5/8 in. diameter, 2-1/4 in. wide impeller with and without housing are shown in Figure 29. The sound power spectra exhibit peaks that are speed independent and correspond to the Helmholtz resonance frequency. Calculations based on Equations (6.7) and (6.9) gave a resonance frequency of 315 Hz. The peaks nearly coincide with this frequency. The average difference between the sound power level produced by the impeller alone and the sound power level produced by the impeller and the housing is nearly 16dB, which agrees with calculations based on Equation (6.9).

6.3 Lumped Impedance Model

The acoustical behaviour of a ducted centrifugal blower may be described by the lumped impedance model. In describing each element of the ducted system, the assumption is made that the wave length of the radiated sound is large compared to the transverse dimensions of the blower system. The lumped impedance model of a ducted blower system has been described by Yeow (Ref. 15); the lumped impedance representations are shown in Figure 30. Since the dimensions of the outlet duct and conical diffuser are comparable to a wave length, they are analyzed separately. In the lumped impedance model each element is represented by a constriction (inductance) or capacitance. The admittance at the throat of a diffuser as shown in Figure 31 is given by

$$Y_4 = \frac{S_4}{\rho_o a_o} \left(\frac{1 - R_4}{1 + R_4} - \frac{1}{kr_4} \right) \qquad (6.11)$$

where the complex reflection factor, $R_4 = R_5 e^{-2ikl}$

and
$$R_5 = \frac{1}{2ikr_5 - 1}$$ (6.12)

and k is the wave number.

r_4 and r_5 are the radius of the diffuser at Sections 4 and 5 respectively

S_4 is the throat area.

k is the wave number.

ρ_o is the density of the ambient air.

The real and imaginary parts of the admittance and complex reflection factor are shown in Figure 32. Both real and imaginary part of the admittance tend rapidly to zero at high frequencies, going through a series of resonances and anti resonances. These occur at diffuser lengths corresponding to the multiples of half wave lengths. The real part of the admittance tends to a constant value with the imaginary part approaching zero at high frequencies.

The outlet duct length is assumed to be infinite and hence its impedance may be represented by $\rho_o a_o$.

Within the demarcation boundary, the neck of the casing behaves like a constricted passage at low frequencies and the impedance is given by

$$\frac{i\rho_o a_o k l_e}{S_4}$$ (6.13)

where l_e is the length of the constriction

and the impedance at Section 3 is given by

$$Z_3 = Z_4 + \frac{i\rho_o a_o k l_e}{S_4}$$ (6.14)

The rotor casing at low frequencies acts like a tank. For long wave lengths

$$Y_{tank} = \frac{i\omega V_o}{\rho_o a_o^2}$$ (6.15)

and the admittance for the complete casing is:

$$Y_2 = Y_3 + Y_{tank}$$ (6.16)

The impedance due to the inlet is

$$Z_1 = \frac{1}{Y_1} = \frac{\rho_o a_o}{\pi a_1^2} \left[\frac{(ka_1)^2}{4} + ik \left(L_1 + l_c + \frac{8a_1}{3\pi} \right) \right]$$ (6.17)

which includes the radiation impedance of the inlet pipe and the impedance due to the constrictive passage of the pipe itself.

l_c is an empirical correction factor for the length of the pipe L_i.

From the above equations, the sound power division ratio between the outlet and inlet side is given by

$$\frac{SWL_2}{SWL_1} = \frac{|Y_1|^2}{|Y_2|^2} \frac{Real\ Y_1}{Real\ Y_2} \tag{6.18}$$

This equation was derived on the assumption that the rotor blade row has no influence on the acoustical behaviour of the system. The rotor blades may act as constrictive passages with inertial reactance to the acoustic flow, or may act like a tank presenting a capacitive reactance, or both. The above expression is not altered if the constrictive rotor impedance is included in the analysis. However, if the capacitive reactance is included the expression in Equation (6.18) changes to,

$$\frac{SWL_2}{SWL_1} = \frac{|Y_1 + \frac{1}{2} Y_R|^2}{|Y_2 + \frac{1}{2} Y_a|^2} \frac{Real\ Y_2}{Real\ Y_1} \tag{6.19}$$

Where $Y_R = \dfrac{i\omega V_R}{\rho_o a_o^2}$

V_R is the volume of the rotor passages.

The numerical values of the sound power division given by Equations (6.18) and (6.19) are shown in Figure 33 along with the experimental measurements. At low frequencies there is reasonable agreement with the measured results, whereas at high frequencies there are large deviations due to drastic simplifications. The maximum around 100 Hz indicates the Helmholtz resonance frequency due to the action of the casing and its neck.

7.0 NOISE MEASUREMENT METHODS

The prime objective of noise measurement is to determine accurately the values of the total sound power levels and the power levels in each of the octave or one-third octave frequency bands. These measurements can be carried out accurately according to the facilities available by any one of the methods, 1) free field 2) reverberant field and 3) in-duct methods.

The free field method requires an anechoic room, which can be very expensive as it requires sound absorbing materials on the walls, floor and ceiling to prevent reflections from the surface. In this method, measurements must be made at a sufficient distance from the face of the duct to be in the far field. If the noise radiation is directional, measurements at close angular intervals enclosing the source over a hemispherical space are required.

In the reverberant field method, a highly reverberant room sufficiently large in relation to the fan dimensions is necessary. The sound power levels are computed by reverberation time measurements in each of the frequency bands. In this method also, a number of measurement points are required to compute the total sound power levels.

Industrial fan and blower noise is normally measured by an in-duct method, as this method is much simpler than either the free field or the reverberant field methods and needs no expensive measurement facilities. Sound power is computed by only one measurement inside the duct. ISO and British standards are available for accurately making the measurements and computing the sound power

levels. The details of the specifications are spelled out in two existing standards, ISO/TC43/SCI/WG3 and BS848. ISO has developed this method for use in air conditioning and ventilating duct systems. This method requires that the test duct be terminated anechoically to prevent sound reflections from the duct end. Sound powers from various fans can thus be compared without any effects from back reactions on the source. Since this method assumes uniform distribution of sound across the duct, its dimensions should be small compared to the smallest wave length desired, to avoid the formation of cross modes.

Figure 34 shows the experimental set-up for measuring the sound power radiated from the exhaust side of a 15 horsepower blower by the in-duct method. The exhaust pipe is 6 in. in diameter and has an anechoic termination with an exponential horn packed with loose fibreglass material with a centre passage for the discharge of the exhaust flow. The exponential horn behaves like an acoustic transformer in matching the impedance from the duct end to the outside in eliminating the duct termination effects. The measuring microphone is located halfway between the wall and the axis of the test duct, and about a diameter away from the throat of the horn. The microphone should contain a slit tube or nose cone to suppress the flow noise due to turbulence.

8.0 NOISE CHARACTERISTICS OF BLOWERS

Engine Laboratory has a wide variety of blowers in operation, ranging in capacity from fractional horsepower to 700 horsepower. The pumping capacities of these blowers vary from 250 lb./sec. at 13-1/2 in H_2O pressure in a 700 hp blower to 1 lb./sec. in a 1/3 hp blower. The impellers vary in size from approximately 6 ft. to 11 in. in diameter. A few of them have forward or backward curved blades but most have straight radial blades. As many of these blowers are installed in test facilities, noise measurements according to the ISO standards specification were difficult and therefore measurements were taken outside the exhaust duct exit at about 4-6 ft. distance from the duct exit. The main objective of these measurements was to study the noise characteristics of the various blowers in order to identify the important frequency components.

A brief description of each blower system and its physical and operating characteristics along with its measured noise spectrum are described below.

700 horsepower blower (manufactured by Canadian Sirocco Co.)

horsepower: 700

rated capacity: 250 lb./sec. at 15-1/2 in. H_2O

100 lb./sec. at 24 in. H_2O

size: approximately 6 ft. in diameter, 15 in. wide on each side of the impeller exit

double inlet, two sets of 12 backward curved blades

length of blades = 9 in.

drive: variable speed DC motor, 700 hp.

The noise spectra for the two speeds of 965 and 403 rpm are shown in Figure 35(a). The characteristics of the spectra indicate broadband noise with peaks at the low frequency end of the spectrum. The blade passing frequency tones should appear in the third octave bands containing frequencies of 193 and 80 Hz for these two speeds. While the figure indicates a suggestion of peaks in these bands, they are not sufficiently sharp and well-defined to be called tones. The spectra are dominated by frequencies below 1000 Hz. The drop in level with increase in frequency corresponds to the 5dB/octave band line as suggested in Reference 4 below 2000 Hz. Above 2000 Hz, the levels decrease much more sharply.

42.5 horsepower fan (Sheldon Engineering Ltd.)

> rated capacity: 7500 cfm at 23 in. H_2O
>
> size: 42-1/2 in. diameter impeller
>
> 9-1/4 in. wide
>
> 14 straight radial blades, approximately 20 in. long
>
> single inlet
>
> 8 variable inlet vanes
>
> drive: 50 horsepower induction motor at 1750 rpm.

The blade passing frequency tone at 400 Hz dominates the noise spectrum in the valve full open condition as shown in Figure 35(b). The noise levels in frequency bands above the blade passing frequency clearly follow the 5dB/octave drop line. The presence of inlet vanes was expected to generate a strong blade passing frequency tone as a result of the wakes shed from the vanes impinging on the impeller blades. Partial closing of the vanes at various settings appears to decrease the tone level, enhancing the levels of broadband noise at frequencies higher than 500 Hz.

40 horsepower blower (Canadian Blower and Forge Company)

> rated capacity: 8000 cfm at 18 in H_2O
>
> size: 30 in. diameter
>
> 5 straight radial blades
>
> single inlet
>
> drive: 40 horsepower induction motor at 1750 rpm.

This blower was located on the roof of the building to supply air to an Engineering Acoustic Facility model. Figure 35(c) shows octave band noise levels with an indication of strong tones at the blade passing frequency and its second and third harmonics in the octave bands at centre frequencies of 125, 250, and 500 Hz respectively. The drop in noise level beyond 500 Hz is much greater than 5dB/octave.

30 horsepower blower (Canadian Blower and Forge Company)

> rated capacity: 8000 cfm at 18 in. H_2O

This blower is being used in the engine icing facility in Cell No. 3. Figure 35(d) shows the noise spectra for a normal inlet and for a 2 in. diameter inlet. At each condition the spectrum is clearly dominated by tones in the 160 and 200 Hz bands. While the blade passing frequency tone is contained in the 160 Hz band, it is difficult to explain the tone in the 200 Hz band as the second harmonic should be in the 300 Hz band. The Helmholtz frequency of the blower housing system may be expected to appear at much lower frequencies. The broadband noise levels are in close agreement with the 5dB/octave band line except at high frequencies. The noise spectra did not appear to change drastically with changing inlet conditions.

15 horsepower blower (Canadian Blower and Forge Company)

> rated capacity: 1500 cfm at 0.9 psi
>
> 2100 cfm at 0 psi

size: 26 in. diameter impeller

10 straight radial blades

1.25 in. wide

inlet flow control through a valve

drive: 15 hp induction motor at 3500 rpm.

With the valve fully open, the predominant noise component appeared to be the tone at the blade passing frequency as shown in Figure 36. Noise levels in the frequency bands below 500 Hz are relatively low, unlike the noise spectrum from other blowers. Partially closing the valve to about the 1/2 open position increased the high frequency component, with the tone at the blade passing frequency disappearing. The broadband noise levels are parallel to the 5dB/octave band line at both conditions.

1-1/2 horsepower blower (Clark Vacuum Cleaner Blower)

rated capacity: 120 cfm at 30 in. H_2O

size: 5-1/2 in. diameter

single stage

8 backward curved blades

0.625 in. wide

tip Mach No. 0.34

drive: universal motor 12,600 rpm.

The blade passing frequency tone occurs at 1600 Hz in Figure 37(a), which is in the most annoying frequency range. The other peak at 400 Hz does not coincide with the fundamental of the rotor frequency. The broadband noise levels are relatively high at frequencies above 400 Hz.

1-1/2 horsepower blower (Woods Vacuum Cleaner Blower)

rated capacity: 120 cfm at 30 in. H_2O

size: 6.2 in. diameter

1.9 in. diameter inlet

8 backward curved blades, double stage

2.15 in. long blades

0.220 in. thick

tip Mach No. 0.34

drive: universal motor, free running speed 15,750 rpm.

The noise characteristic of this blower in Figure 37(b) is similar to that of the previous one; the blade passing frequency tone at 2000 Hz is dominant with another peak around 200 Hz, which coincides with the fundamental of the rotor frequency. Unlike the characteristic of the previous blower, the lower frequency bands do not contain significant sound energy.

1-1/2 horsepower fan (Canadian Blower and Forge Ltd.)

size: 12 in. diameter

10 straight radial blades, 3 in. long

4-7/8 in. diameter inlet with circular scroll around the impeller.

Figure 37(c) shows that with the normal inlet the noise spectrum is dominated by the tone at the blade passing frequency with an indication of a peak at the second harmonic. With the inlet partially blocked by a 1 in. diameter hole, the blade passing frequency tone became less conspicuous with some decrease in broadband noise levels in the lower frequency end.

1/3 horsepower blower (Sheldon Engineering Ltd.)

       rated capacity: 650 cfm at 0 psi

       size: 11 in. diameter

             12 backward curved circular arc blades

             2 in. length

             5-7/16 in. diameter inlet

             5-1/2 in. diameter outlet pipe

       drive: 1/3 horsepower induction motor at 1700 rpm.

Figure 37(d) shows no evidence of any tone at the blade passing frequency, but the spectrum at the fully open inlet condition is dominated by a tone at 160 Hz and a peak of 200 Hz. The cause of the tone at 160 Hz may be attributed to the presence of six struts supporting the 12 blades. The tone in the 200 Hz band may be ascribed to the characteristic frequency associated with the casing geometry, which is the Helmholtz resonance frequency. Partially blocking the inlet with a 1 in. diameter hole removed this peak and reduced the broadband noise over the entire frequency range.

9.0 FURTHER AREAS OF RESEARCH

(1) It has been established that the tones at the blade passing frequency and its higher harmonics are produced by the impingement of the flow leaving the impeller blade exit on the cut off edge formed by the junction of the volute casing with the exhaust duct. Increasing the distance of the cut off edge from the blade exit reduces these levels. It would be useful to investigate the effect on the aerodynamic and acoustic performance of the impeller of eliminating the volute casing and replacing it with a collector with two circular end plates enclosing the impeller.

(2) Theoretical investigations in Reference 16 have shown that uneven spacing of the blades reduces the tone at the blade passing frequency by increasing the levels in the side bands, thus lowering the annoying quality of the sound. Some of the cooling fans used in automobiles (mainly axial flow fans) are designed with uneven blade spacings for reducing the noise. As the tone at the blade passing frequency appears to be the prominent noise component, unequal blade passages may be expected to reduce this peak tone in centrifugal fans. However, the effect on the aerodynamic performance of the fan must be understood and balanced against possible acoustic benefits.

(3) Investigations by Fowler (Refs 17, 18) have revealed that the use of aerofoil blades instead of thin curved blades improves the flow within the blade passages, with improved aerodynamic performance. The presence of slots in the blades has been shown to delay flow detachment by improving the flow distribution and stability. As instability of the flow and turbulence are among the major causes of random noise generation, it is worthwhile making a comparative assessment of the noise and aerodynamic performance of a fan with three different sets of blades, viz thin plate curved blades, aerofoil blades, and blades with slots.

(4) Noise characteristics cannot be explained by aerodynamic sources alone and it has been shown that the casing and ducted environment exert a powerful influence on noise characteristics. Most of the work in this area presented in this report is based on low frequency

approximation which fails to explain the behaviour of the ducted environment at the middle and high frequency range of the noise spectrum. Analytical work leading to ducted system behaviour at higher frequencies would be very useful, since most of the spectra contain significant levels above 200 Hz.

10.0 CONCLUSIONS

(1) The blade passing frequency tone and its harmonics are shown to be generated by the interaction of the flow issuing from the blade exit with the cut off edge. By locating the cut off at the optimum distance from the blade tip, significant reductions in tone levels can be obtained. Broadband noise is generated by the unsteady flow processes within the impeller blade passages.

(2) A rough estimation of broadband noise levels may be obtained by the available empirical equations, but they fail to predict the tone levels with any significant accuracy.

(3) Fan noise laws have been derived from similarity principles. A wide range of variations exists in regard to the dependence of sound power levels on the exponents of impeller speed and diameter. The non-dimensional numbers — Mach number, Reynolds number, Strouhal number, and flow coefficient — exert significant influence on noise generation, but the noise levels show strong dependence on flow coefficient.

(4) The volute casing and the ducted environment exert a powerful influence on noise characteristics. The behaviour of ducted fans may be described by the treatment of fans as black boxes, as applied to the communication networks and the lumped impedance model. The ability of these methods to give reliable predictions ought to be further exploited. The lumped impedance model has given reasonable agreement only at low frequencies.

(5) Among the various blowers tested, the prominent noise component appears to be the tone at the blade passing frequency. There were two exceptions: the noise characteristic of a large blower was predominantly broadband, but a 1/3 horsepower blower indicated the presence of a tone due to the struts supporting the rotor blades.

(6) The promising areas of research appear to be:

    (i)   elimination of the volute casing and replacing it by a collector casing,

    (ii) unequal blade passages,

    (iii) use of aerofoil and slotted blades, and

    (iv) analytical work leading to the ducted system behaviour at high frequencies.

11.0 REFERENCES

1. Fowler, H.S.

    An Investigation of the Flow Processes in a Centrifugal Compressor Impeller.
NRC, Mechanical Engineering Report ME-220, July 1966.

2. Chanaud, R.C.

    Aerodynamic Sound from Centrifugal Fan Rotors.
Journal of Acoustical Society of America. Vol. 37, 1965, pp. 969-974.

3. Embleton, T.F.W.

    Experimental Study of Noise Reduction in Centrifugal Blowers.
Journal of Acoustical Society of America. Vol. 35, 1963, pp. 700-705.

4. Beranek, L.L.
   Kamperman, G.W.
   Allen, C.H.
   Noise of Centrifugal Fans.
   Journal of Acoustical Society of America, Vol. 27, 1955, pp. 217-219.

5. Baade, P.F.
   Accuracy Considerations in Fan Sound Measurements.
   American Society of Heating, Refrigeration and Air Conditioning Engineers, Transactions, 74th Annual Meeting Preprint, 1967.

6. Madison
   Fan Engineering (Handbook), Buffalo Forge Company, Buffalo, U.S., 1949.

7. Neise, W.
   Application of Similarity Laws to the Blade Passage Sound of Centrifugal Fans.
   Journal of Sound and Vibration, Vol. 43, 1975, pp. 61-75.

8. Maling, G.C.
   Dimensional Analysis of Blower Noise.
   Journal of Acoustical Society of America, Vol. 35, 1963, pp. 1556-1564.

9. Deeprose, W.M.
   Brooks, J.M.
   Effect of Scale on Fan Noise Generation.
   N.E.L. Report No. 512, May 1972.

10. Weidemann J.
    Analysis of the Relation Between Acoustic and Aerodynamic Parameters for a Series of Dimensionally Similar Centrifugal Fan Rotors.
    NASA-TT-F-13798, 1971.

11. Mellin, R.C.
    Selection of Minimum Noise Fans for a Given Pumping Requirement.
    Noise Control Engineering, Vol. 4, No. 1, January-February, 1975, pp. 35-45.

12. Cremer, L.
    The Treatment of Fans as Black Boxes.
    Journal of Sound and Vibration, Second Fairey Lecture, Vol. 16, 1971, pp. 1-15.

13. Wollherr, H.
    Zweitormessungen an einem Radialventilator-Model
    Forschungsvereiniguing für Forschungsberichte 7, 19, 1970.

14. Moreland, J.B.
    Housing Effects on Centrifugal Blower Noise.
    Journal of Sound and Vibration, Vol. 36(2), 1974, pp. 191-205.

15. Yeow, K.W.
    Acoustical Modelling of Ducted Centrifugal Rotors 11, Lumped Impedance Model.
    Journal of Sound and Vibration, Vol. 32(2), 1974, pp. 203-226.

16. Ewald, D.
    Pavlovic, A.
    Bollinger, J.G.
    Noise Reductions by Applying Modulation Principles.
    Journal of Acoustical Society of America, Vol. 49, 1971, pp. 1381-1385.

17. Fowler, H.S.
    Comparison of Thin Plate and Thick Aerofoil Blades in a Centrifugal Fan.
    NRC, Mechanical Engineering Report ME-238, August 1971.

18. Fowler, H.S.
    Unpublished Work.

19. Agnon, R.
    Bartenwerber, M.
    Gikadi, T.
    Neise, W.
    Noise Reduction Methods in Centrifugal Fans.
    Inter-Noise 76 Proceedings, 1976.

20. Yeow, K.W.
    Acoustical Modelling of Ducted Centrifugal Rotors, 1) The Experimental Acoustic Characteristics of Ducted Centrifugal Rotors.
    Journal of Sound and Vibration Vol. 32(1), 1974, pp. 143-152.

21. Ploner, B.
    Herz, F.
    New Design Measures to Reduce Siren Tones Caused by Centrifugal Fans.
    Brown Boveri Revue 56, 1969, pp. 280-287.

22. Maroti, L.A.
    Pradhan, A.V.
    Noise Generation Characteristics of High Speed Centrigugal Fans.
    ASME 69-WA/FE-9, 1969.

23. Csanady, G.T.
    Theory of Turbomachines.
    McGraw-Hill Book Company, 1964.

24. Mugridge, B.D.
    Noise Characteristics of Axial and Centrifugal Fans as Used in Industry.
    Literature review in The Shock and Vibration Digest, May 1975.

CUT OFF EDGE

BLOWER CASING

BLADES
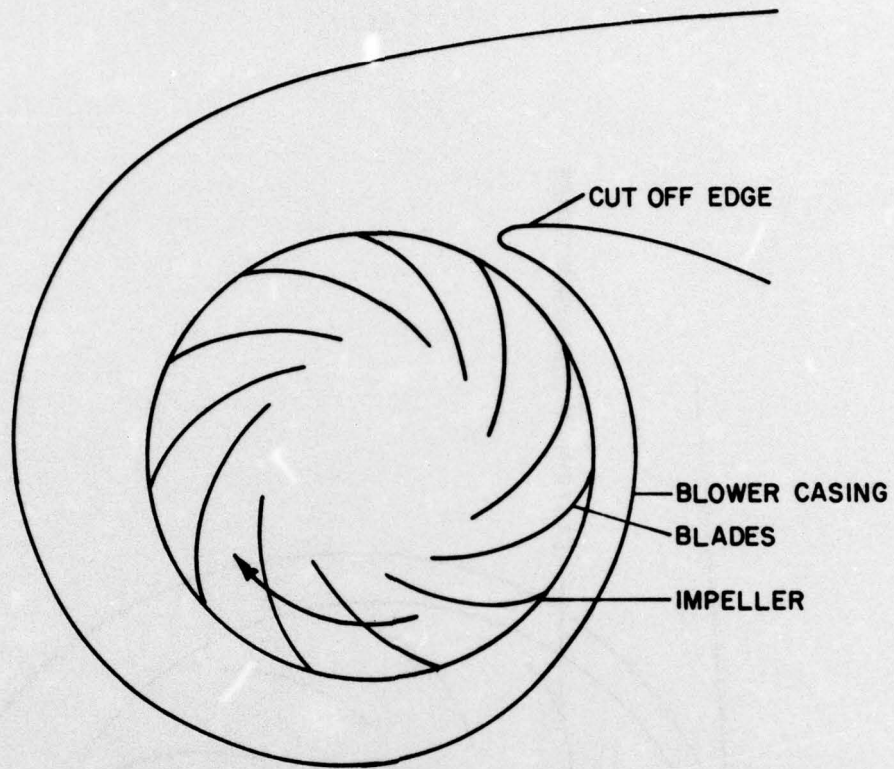
IMPELLER

FIG. 1: CENTRIFUGAL BLOWER

$\beta_2 > 90°$ $\beta_2 = 90°$ $\beta_2 < 90°$
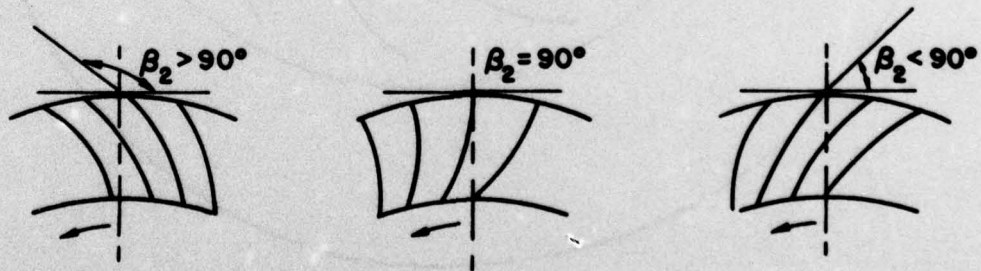
FIG. 2: FORWARD-CURVED, RADIAL AND BACKWARD CURVED IMPELLERS

STATIONARY DIFFUSER VANES
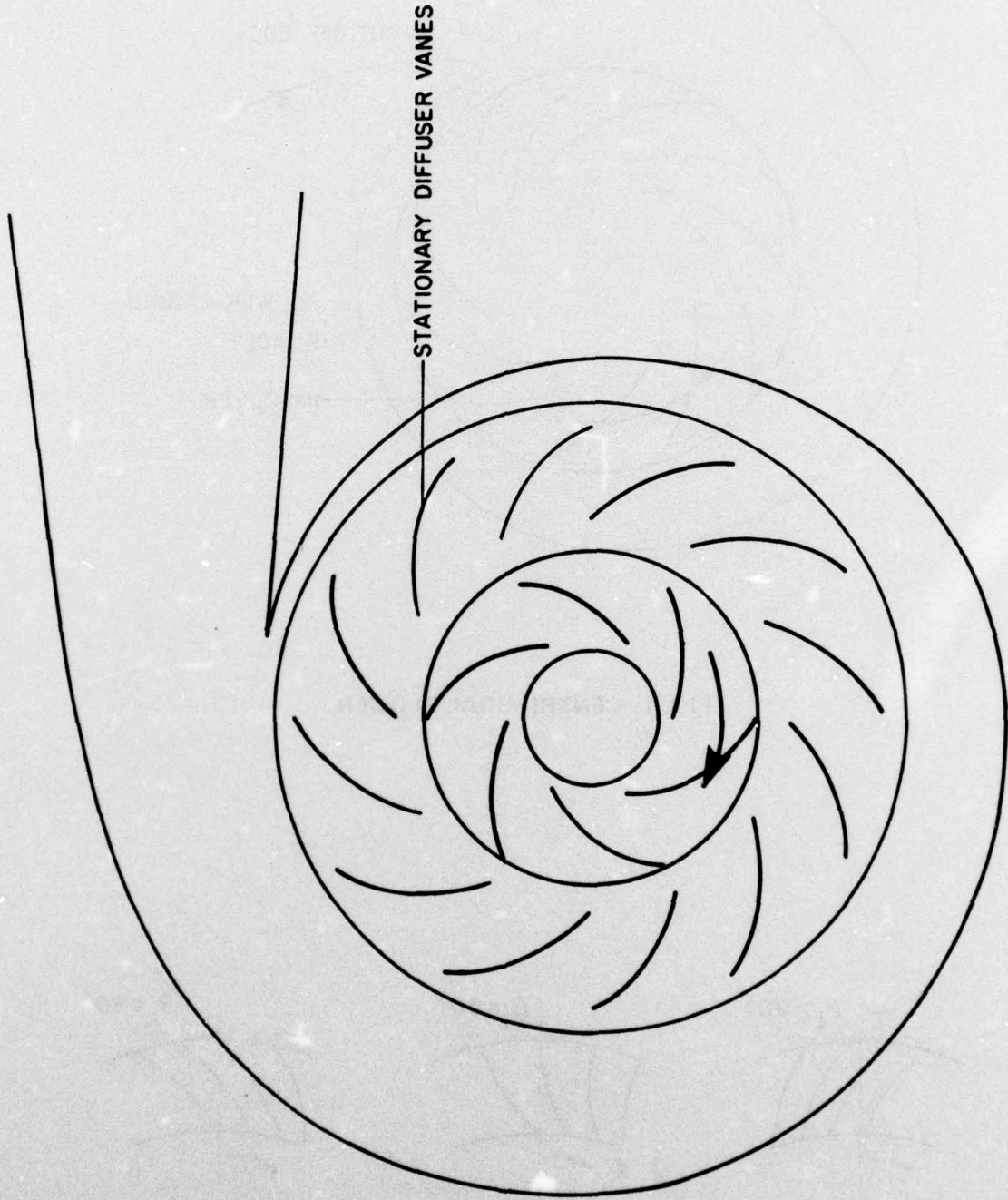
FIG. 3: VOLUTE WITH VANED DIFFUSER
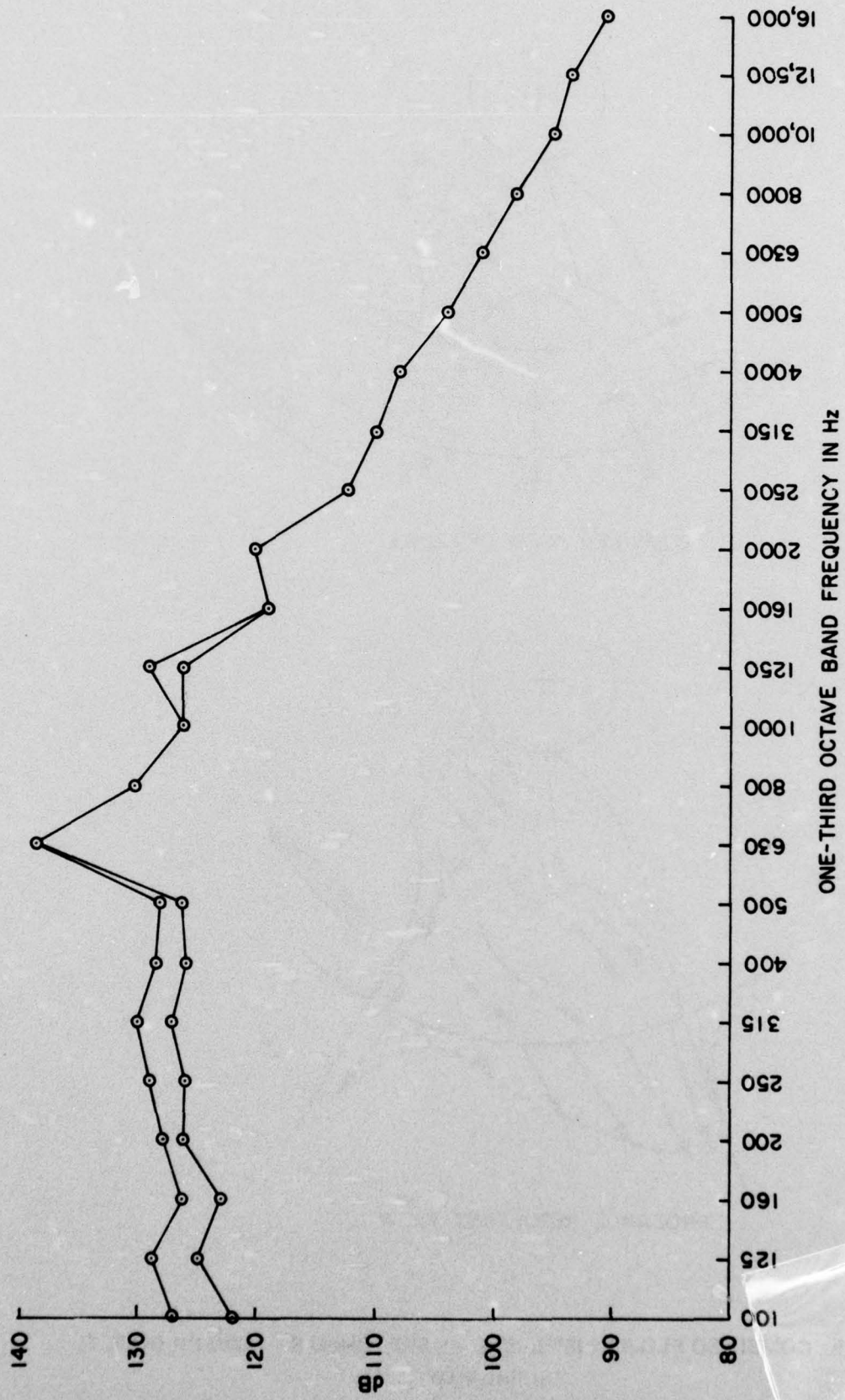
FIG. 4: NOISE SPECTRUM FROM A 15 HP BLOWER
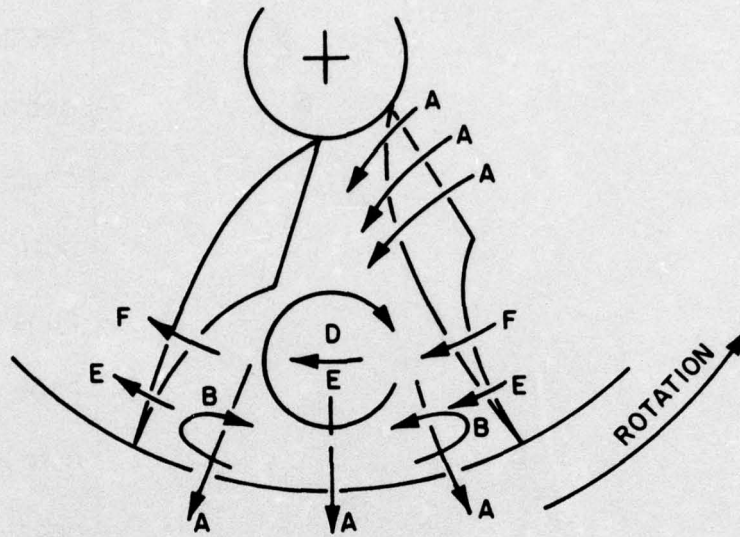
COMBINED VIEW OF FLOWS
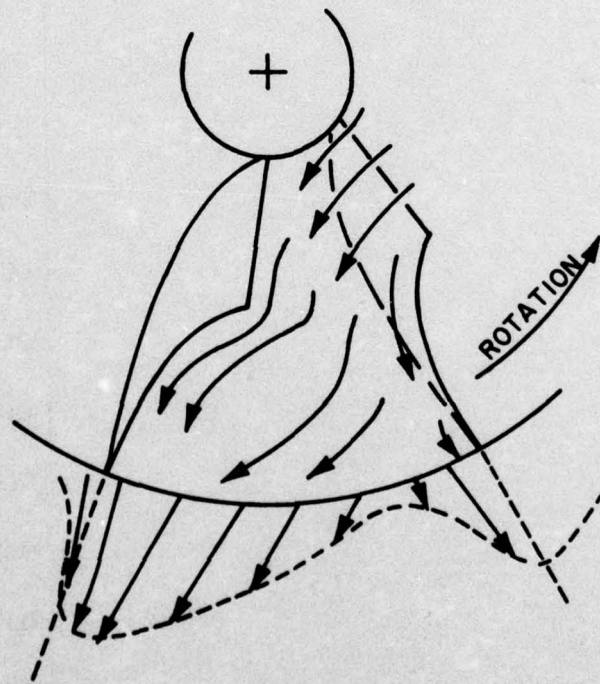
PROBABLE RESULTANT FLOW

FIG. 5: COMBINED FLOW IN IMPELLER AS SKETCHED BY FOWLER (REF. 1)
AXIAL VIEW
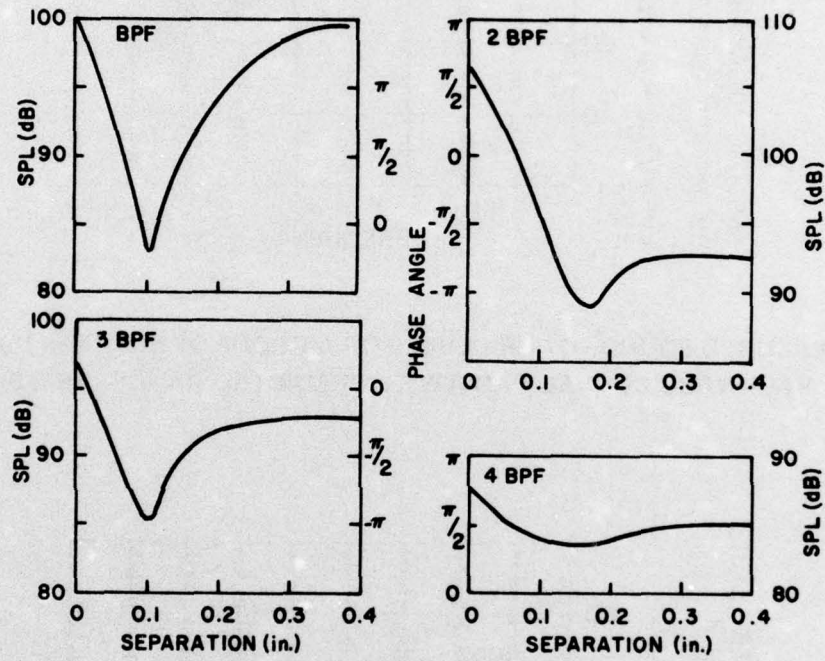
FIG. 6: EFFECT OF CUT OFF CLEARANCE ON BLADE PASSING FREQUENCY TONES (REF. 3)

SPECIFIC DISCHARGE SOUND POWER LEVEL, DB RE 10^{-12} WATT/CFM (INCH W.G.)^2

$Lw_{SD} = \int Lw - 10 \, Log_{10} \, Q - 20 \, Log_{10} P_S$

RANGE PREDICTED
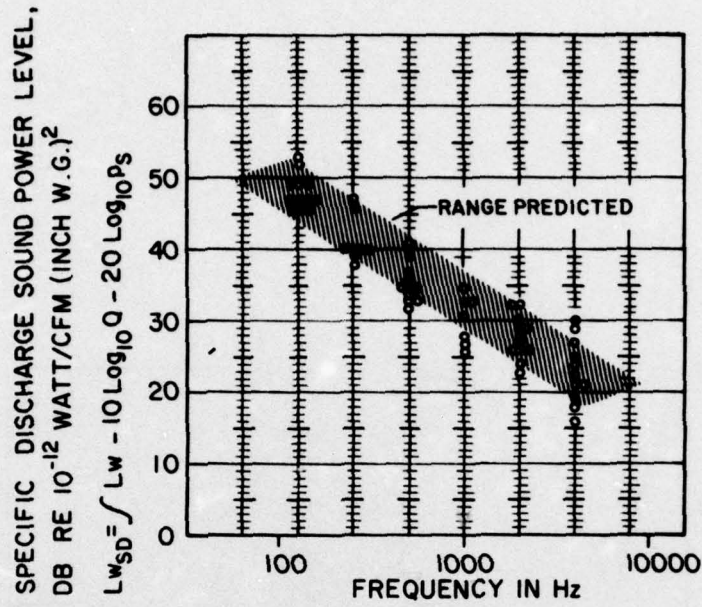
FREQUENCY IN Hz

FIG. 7: MEASURED SOUND POWER LEVELS OF A GROUP OF SIX FANS (EXCLUDING BACKWARD CURVED FANS) WITH PREDICTED RANGE (REF. 5)

SPECIFIC DISCHARGE SOUND POWER LEVEL, DB RE 10^{-12} WATT/CFM (INCH W.G.)^2

$\int Lw_{SD} = \int Lw - 10 \, Log_{10} \, Q - 20 \, Log_{10} P_S$

RANGE PREDICTED
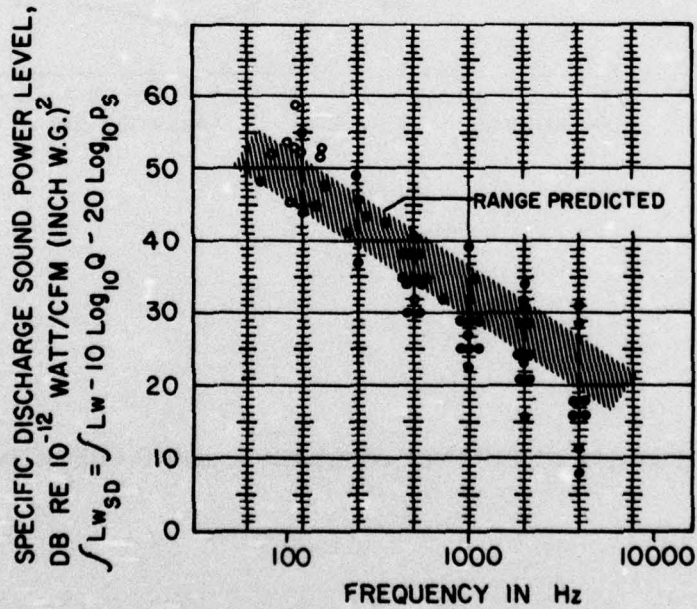
FREQUENCY IN Hz

○ BAND CONTAINING BLADE PASSING FREQUENCY

● ALL OTHER OCTAVE BANDS

FIG. 8: MEASURED SOUND POWER LEVELS OF A GROUP OF EIGHT FANS WITH BACKWARD CURVED BLADES WITH PREDICTED RANGE (REF. 5)
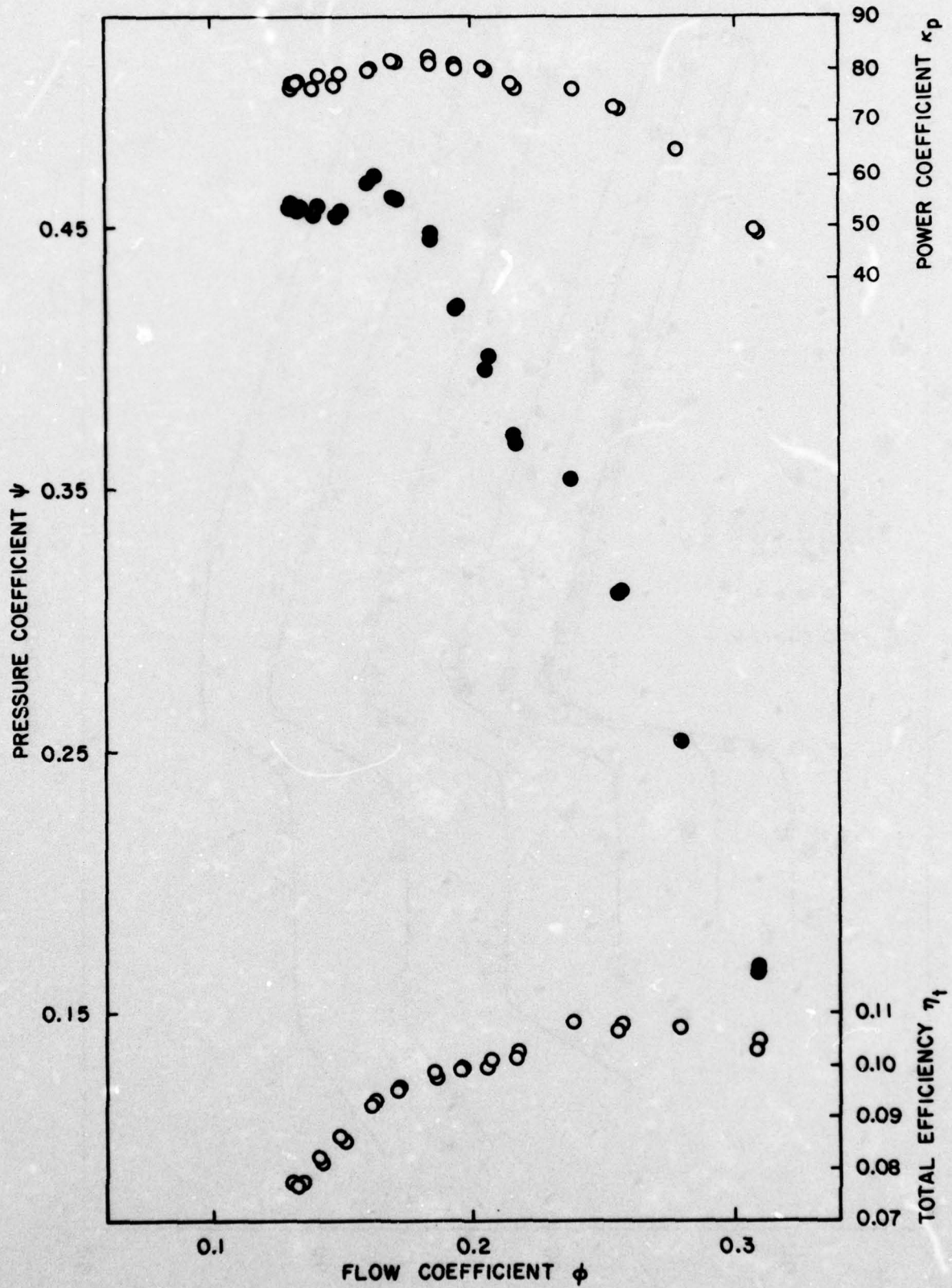
FIG. 9: CHARACTERISTIC OF 0.4437 m DIAMETER FAN AT 2000 rev./min., n_s = 1.466 SET (REF. 9)
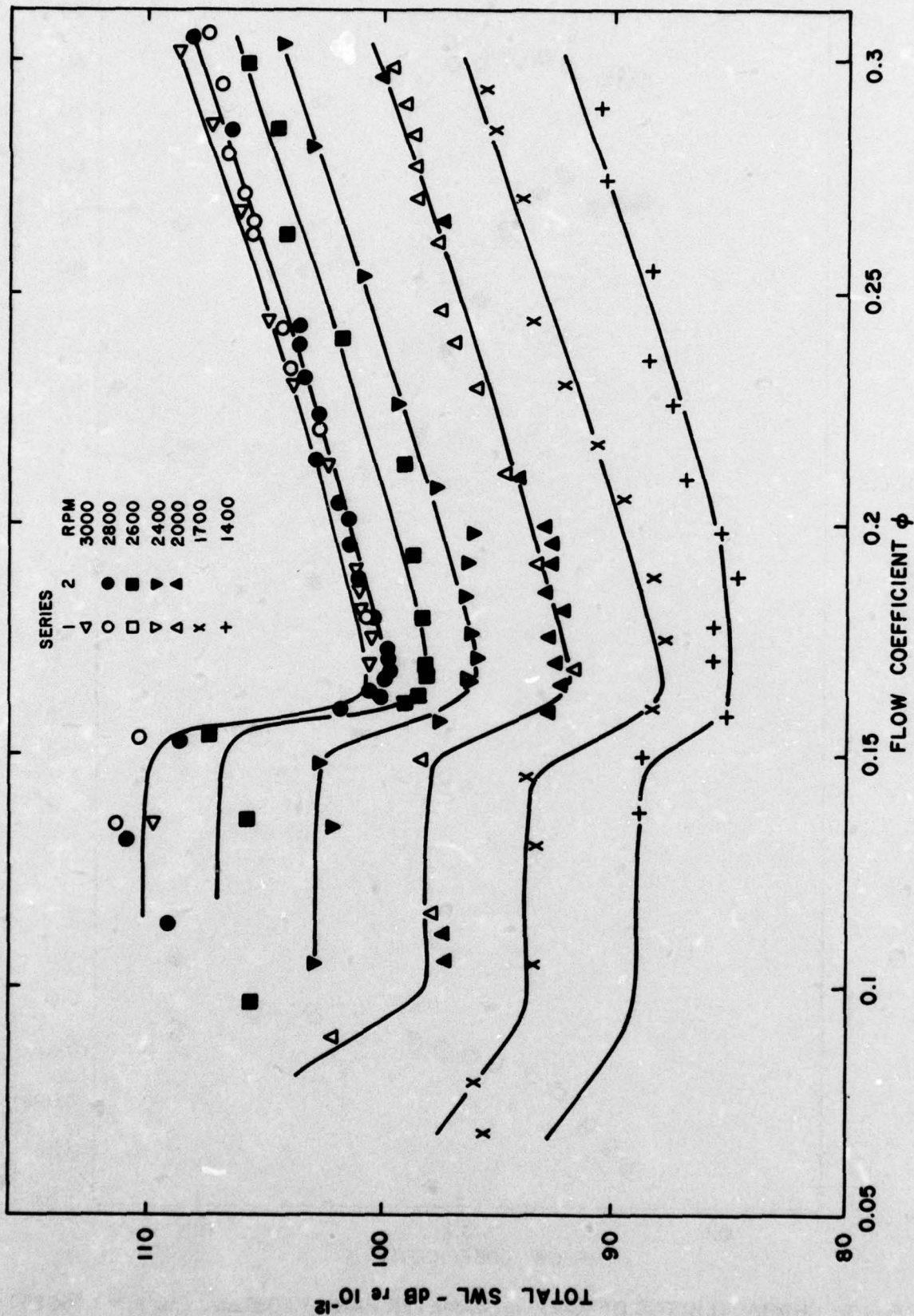
FIG. 10: TOTAL SWL AGAINST FLOW COEFFICIENT 0.4437 m DIAMETER FAN, n_s = 1.466 SET
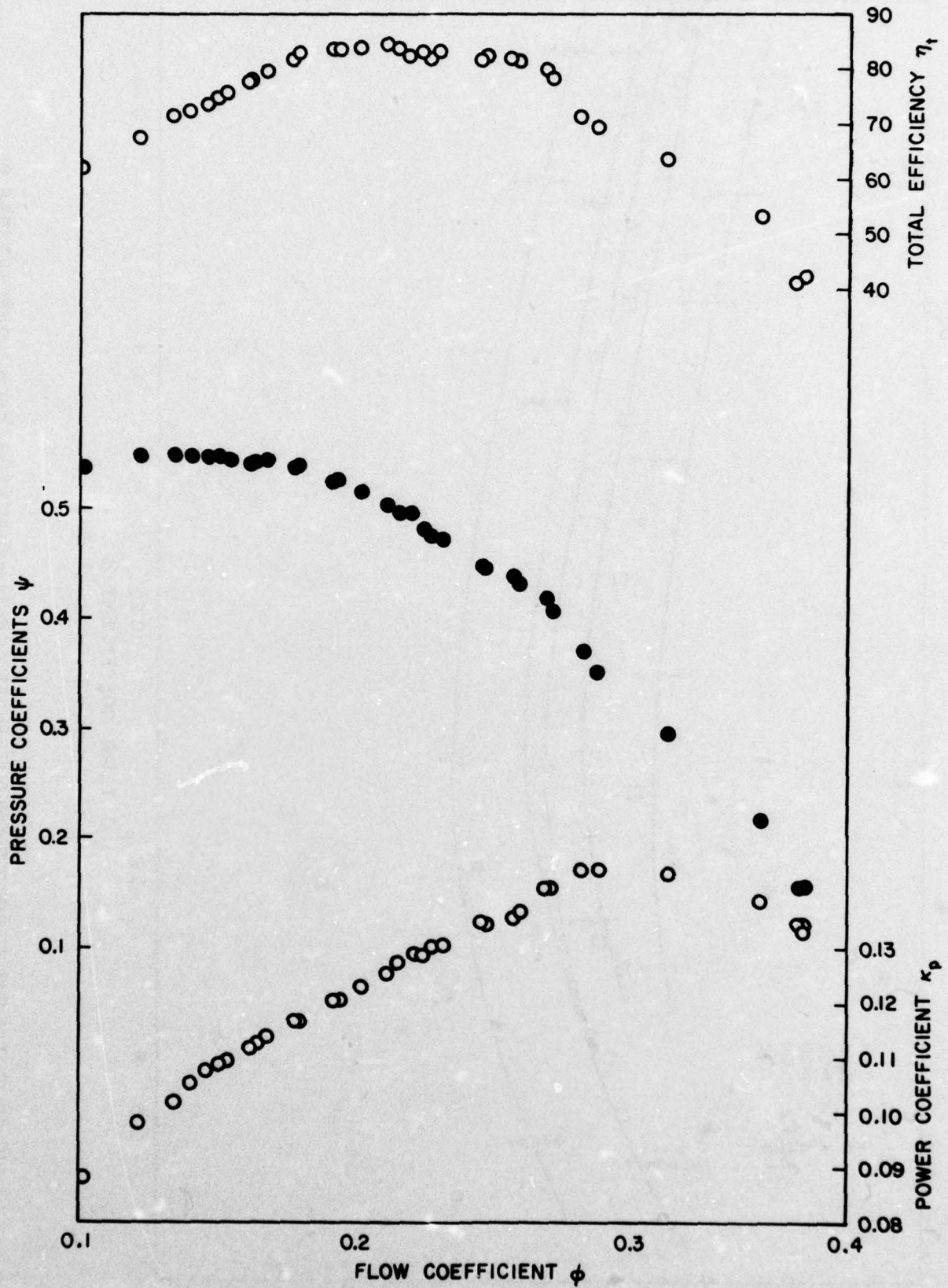
FIG. 11: CHARACTERISTIC OF 1.1552 m DIAMETER FAN AT 750 rev./min., n_s = 0.822 SET
(REF. 9)
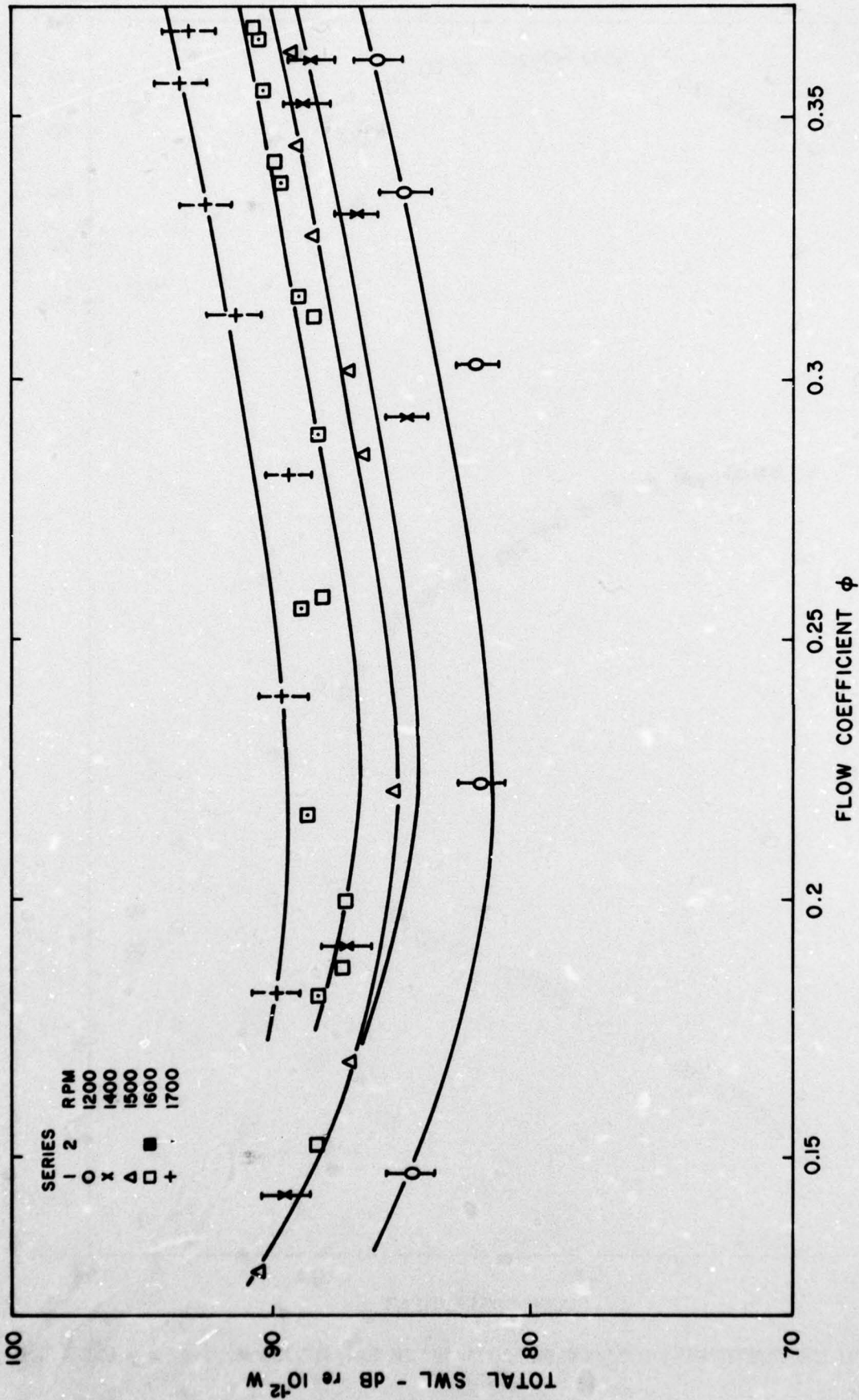
FIG. 12: TOTAL SWL AGAINST FLOW COEFFICIENT 0.4674 m DIAMETER FAN, n_s = 0.822 SET (REF. 9)
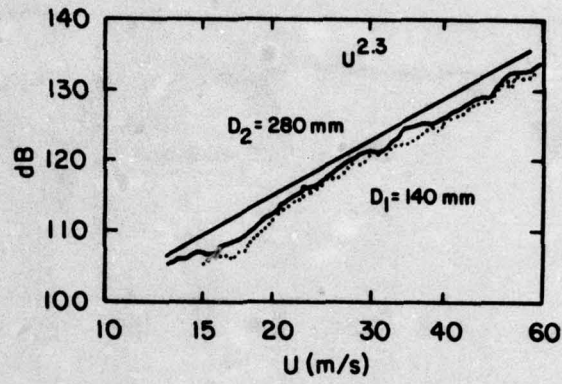
FIG. 13: OVERALL SOUND PRESSURE LEVELS AS A FUNCTION OF IMPELLER TIP SPEEDS
(REF. 7)
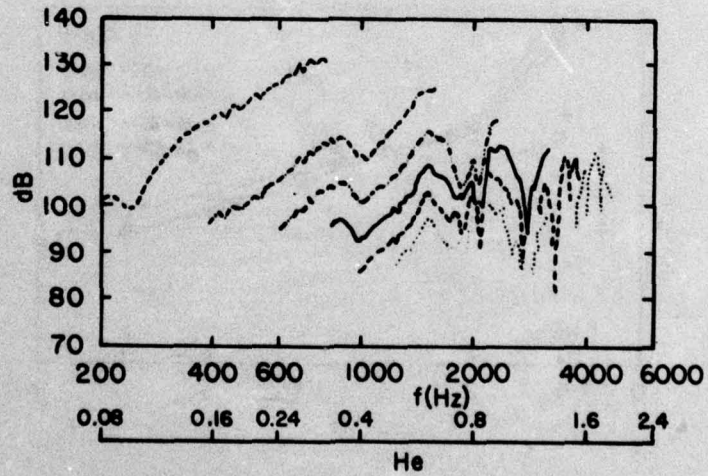
FIG. 14: SOUND PRESSURE LEVELS AT CONSTANT STROUHAL NUMBERS (REF. 7)
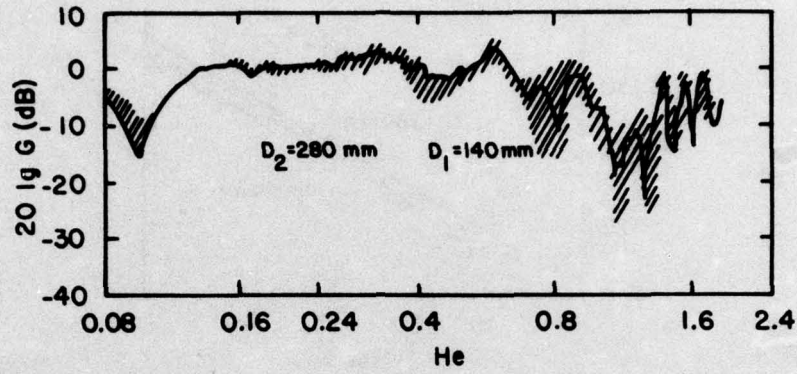
FIG. 15: COMPARISON OF ACOUSTIC FREQUENCY RESPONSE FUNCTION OF TWO FANS
(REF. 7)
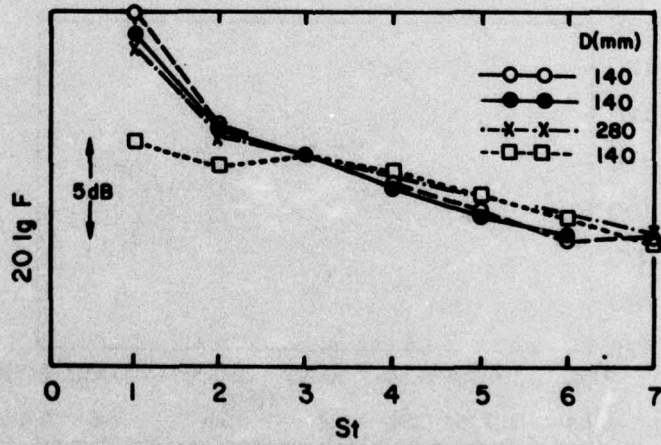
FIG. 16: COMPARISON OF SPECTRAL DISTRIBUTION FUNCTIONS FOR DIFFERENT FANS
(REF. 7)
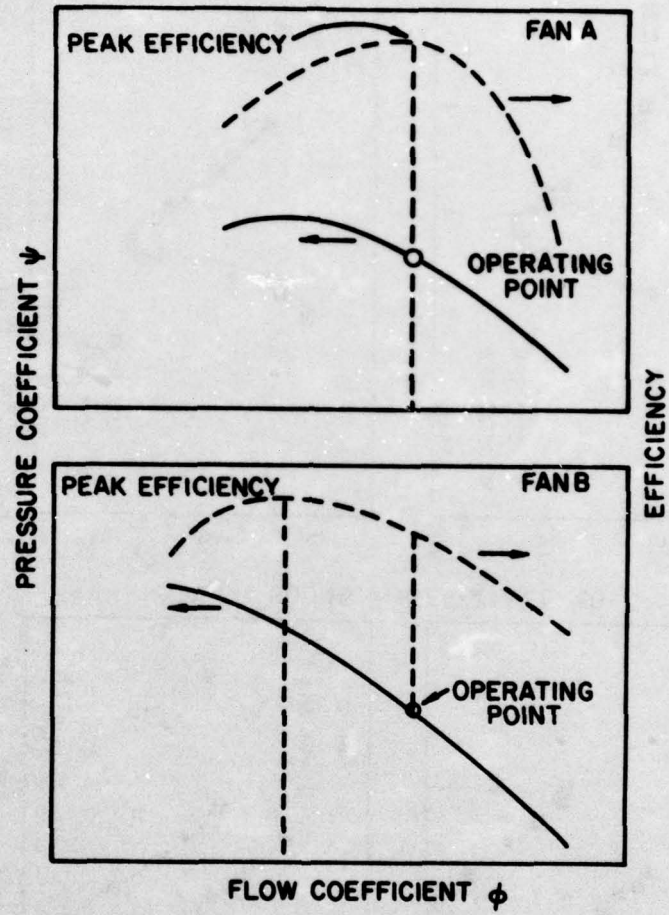
FIG. 17: FAN SYSTEM OPERATING POINT
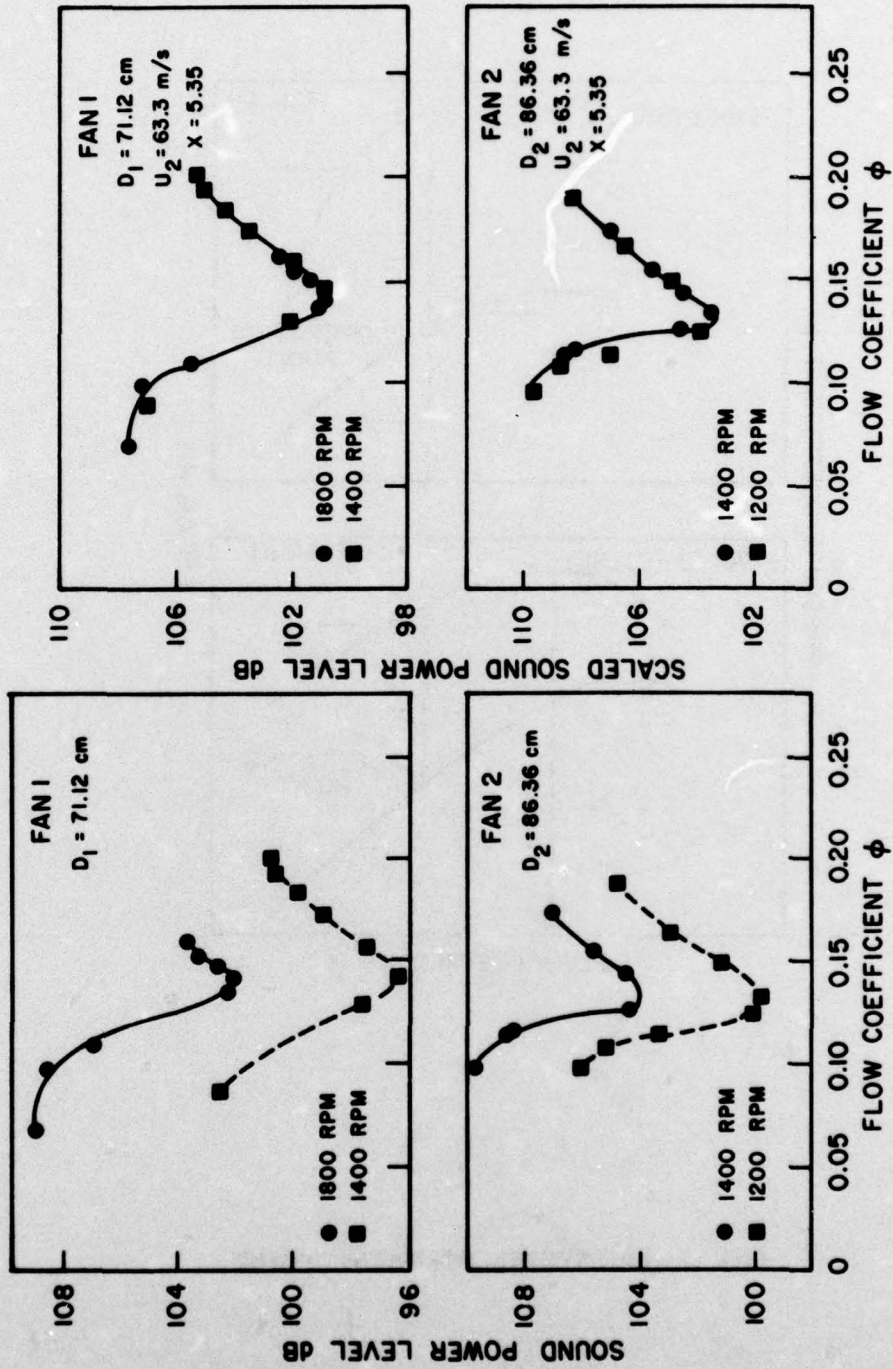
FIG. 18: SCALING OF FAN NOISE WITH RESPECT TO TIP SPEED (REF. 11)
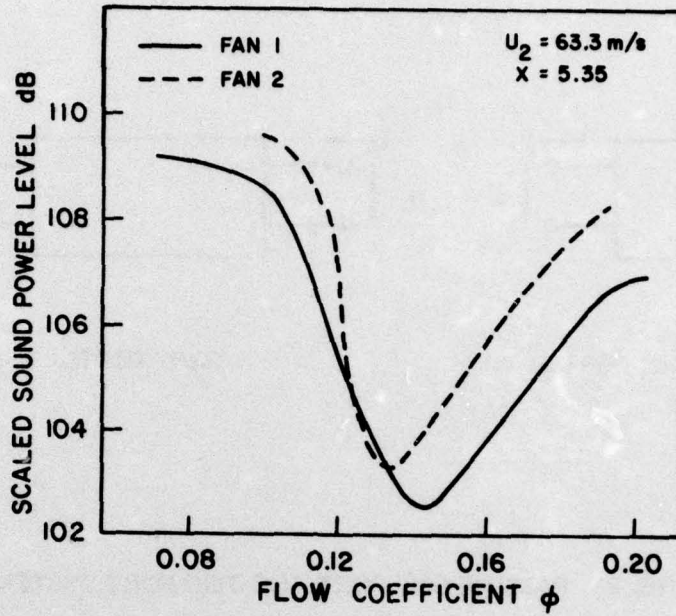
FIG. 19: SCALING OF FAN NOISE WITH RESPECT TO TIP DIAMETER (REF. 19)
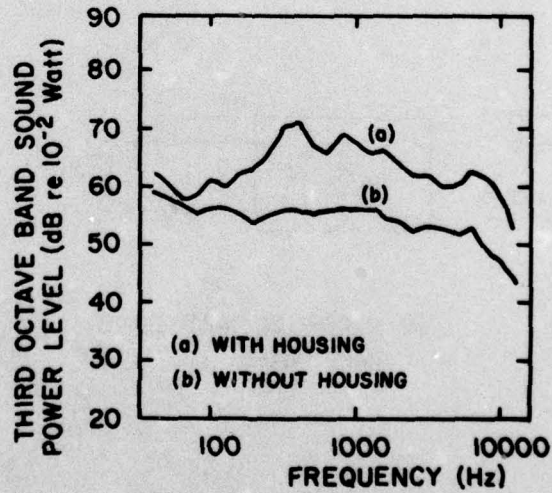
FIG. 20: HOUSING EFFECTS ON IMPELLER NOISE
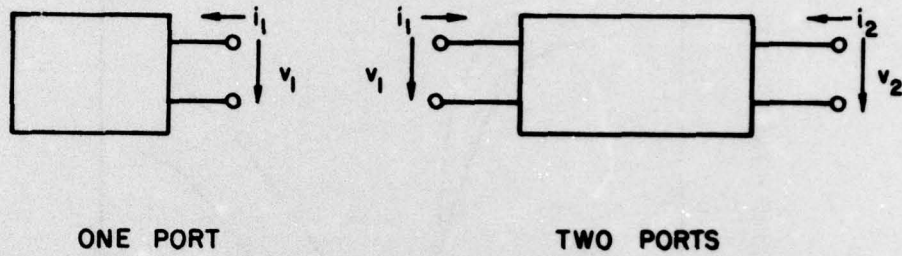
FIG. 21: PASSIVE ONE PORT AND TWO PORT SYSTEMS

(a) VOLTAGE v OR
CURRENT i IS
KNOWN

(b) INTERNAL AND LOAD
IMPEDANCE

(c) EQUIVALENT
ADMITTANCE
REPRESENTATION
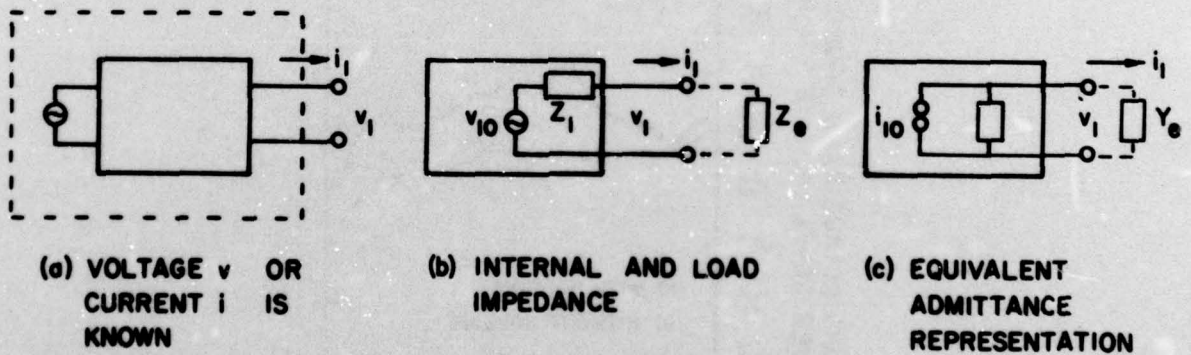
FIG. 22: ACTIVE ONE PORT BOXES
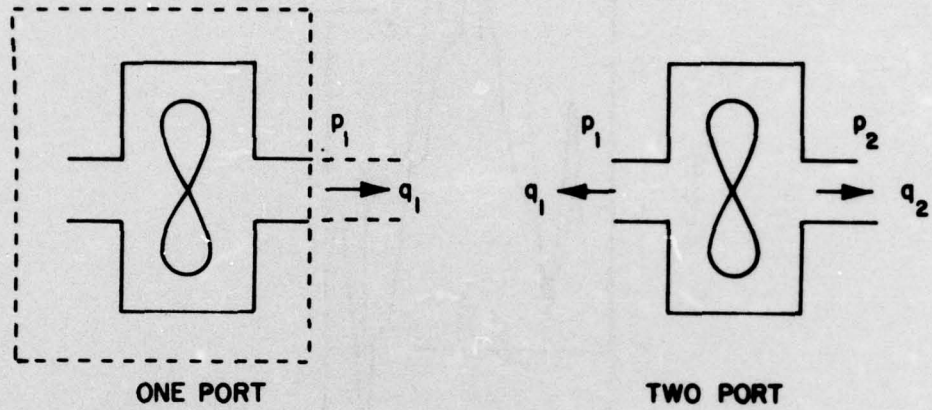
FIG. 23: ANALOGUE REPRESENTATIONS OF A FAN
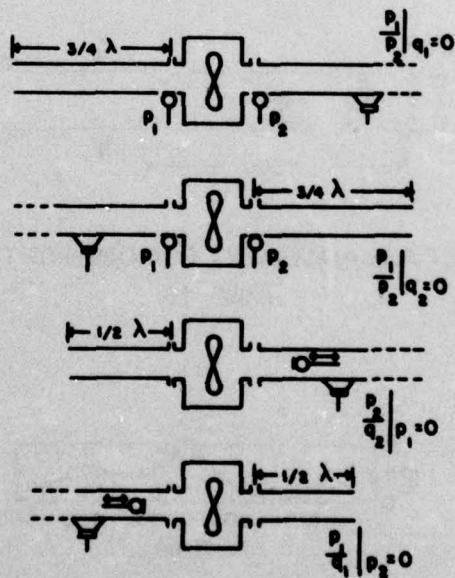
FIG. 24: WOLLHERR'S SCHEMATIC TEST ARRANGEMENTS FOR DETERMINING THE
TWO PORT PARAMETERS OF CENTRIFUGAL FANS (REF. 12)
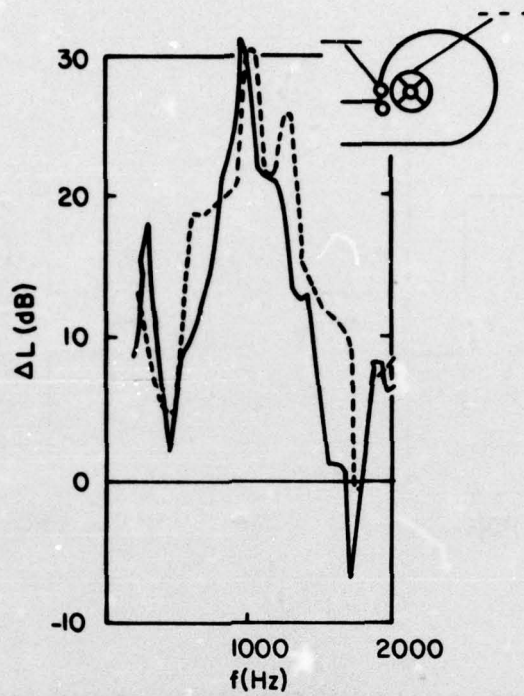
FIG. 25: PEAK SOUND PRESSURE LEVEL DIFFERENCE BETWEEN OUTLET AND INLET.
————, MEASURED WITH ARTIFICIAL MOMENTUM SOURCE;
------, MEASURED WITH ROTATING WHEEL (REF. 12)
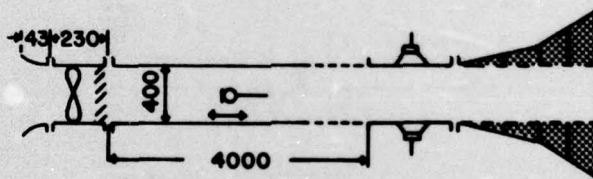
FIG. 26: SCHEMATIC TEST ARRANGEMENT FOR ONE PORT SYSTEM MEASUREMENTS
(REF. 12)
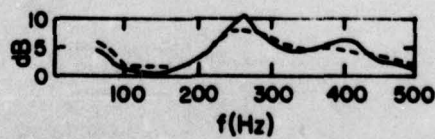
FIG. 27: RESULTS OF MEASUREMENTS ON A FULL-SCALE AXIAL FAN, USING THE
ONE PORT FAN SYSTEM TEST RIG (REF. 12)

OUTLET
M_{A2}

U_0

CAVITY
C_A

INLET
M_{A1}

I_0

C_A

M_{A2}

R_A

SINGLE INLET

OUTLET
M_{A2}

U_0

CAVITY
C_A

INLET M_{A1}

INLET M_{A1}

I_0

C_A

M_{A1} M_{A1} M_{A2}

R_A

DOUBLE INLET

ACOUSTICAL MODEL   ELECTRICAL ANALOGUE
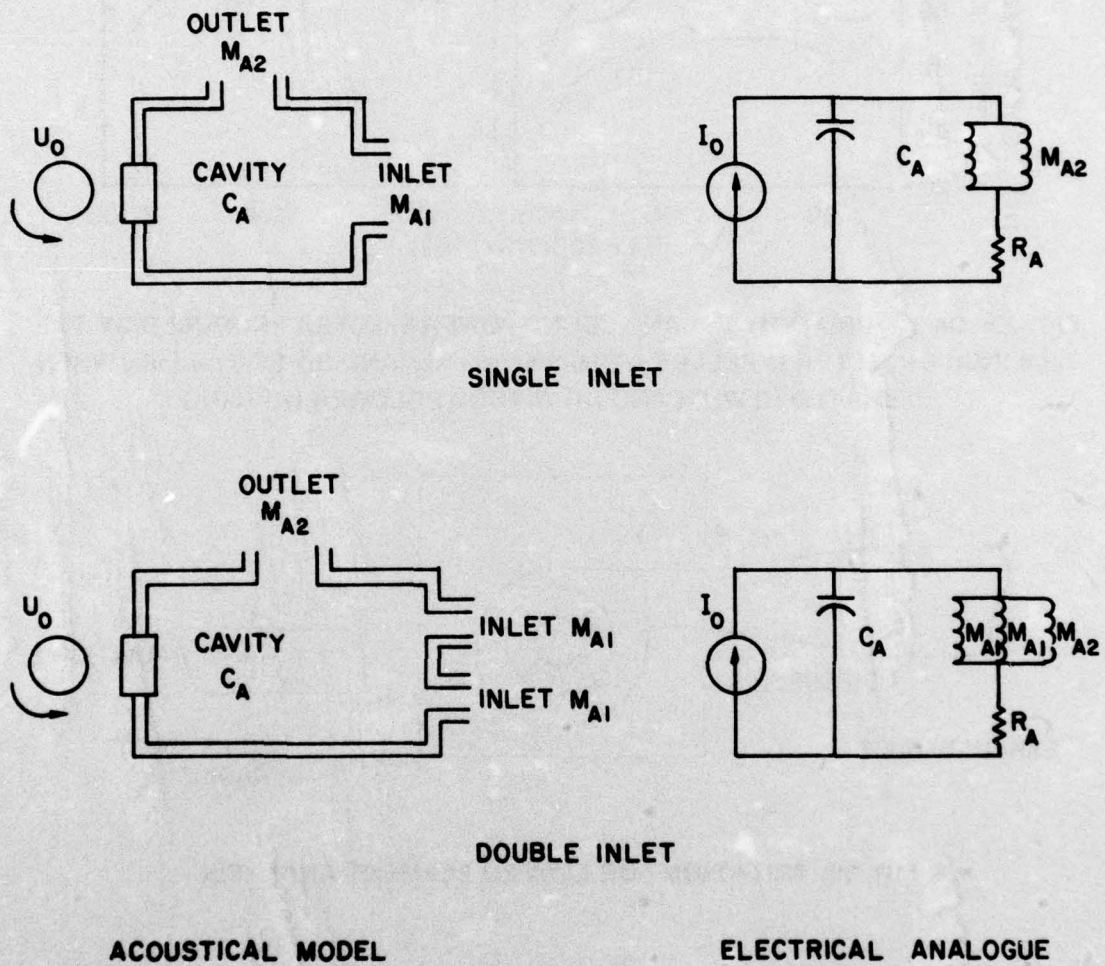
FIG. 28: ACOUSTICAL MODELS AND ELECTRICAL ANALOGUE OF SINGLE AND DOUBLE
INLET BLOWERS
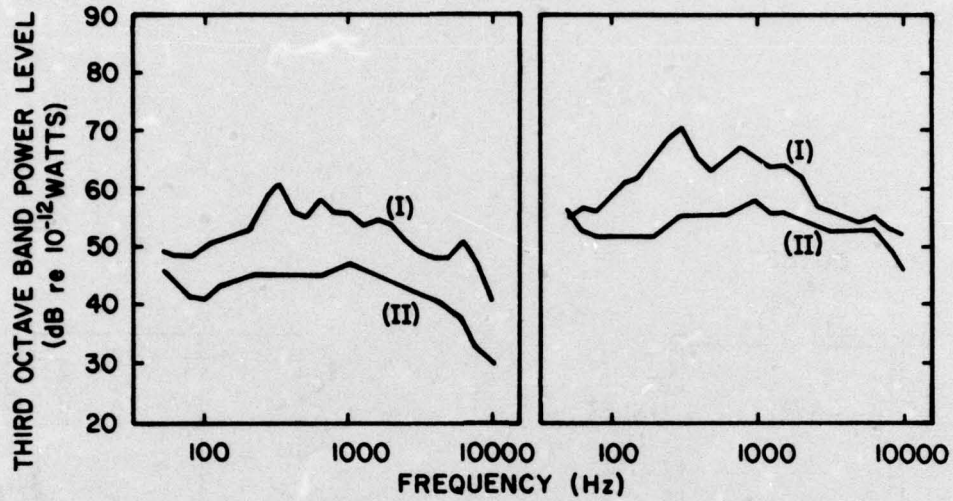
FIG. 29: ONE-THIRD OCTAVEBAND SOUND POWER SPECTRA PRODUCED BY THE 7-5/8 INCH DIAMETER IMPELLER AT (a) 900 rev./min. AND (b) 1400 rev./min. WHEN OPERATED (I) WITH AND (II) WITHOUT BLOWER HOUSING
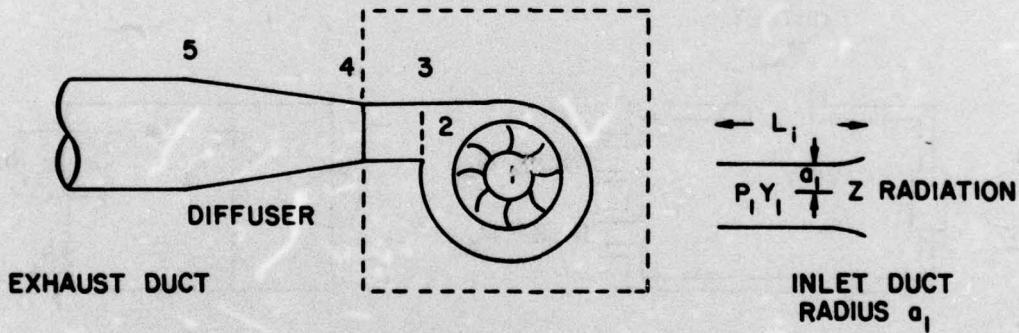
FIG. 30: NOTATION FOR LUMPED ELEMENT ANALYSIS
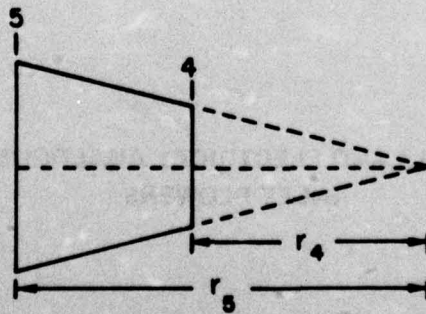
FIG. 31: DIFFUSER
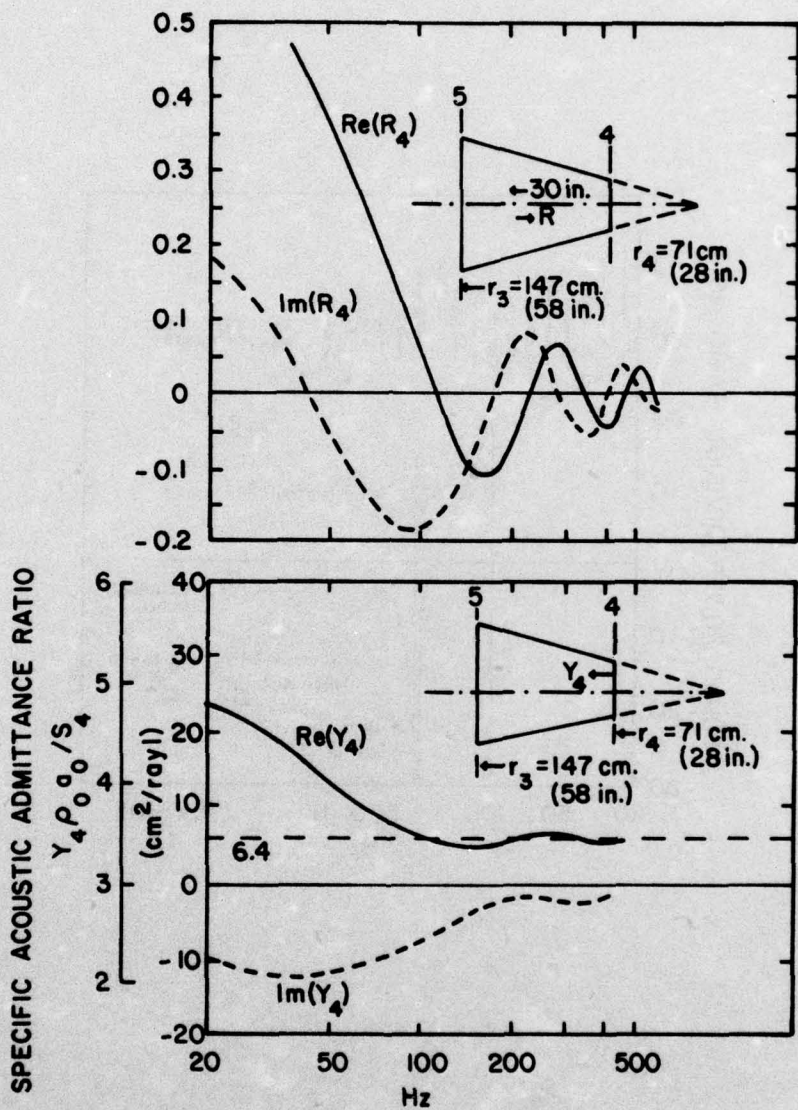
FIG. 32: (a) REAL AND IMAGINARY PARTS OF COMPLEX REFLECTION FACTOR R_4 IN DIFFUSER HORN. (b) REAL AND IMAGINARY PARTS OF ANALOGOUS ADMITTANCE Y_4 AT THROAT OF HORN (REF. 15)
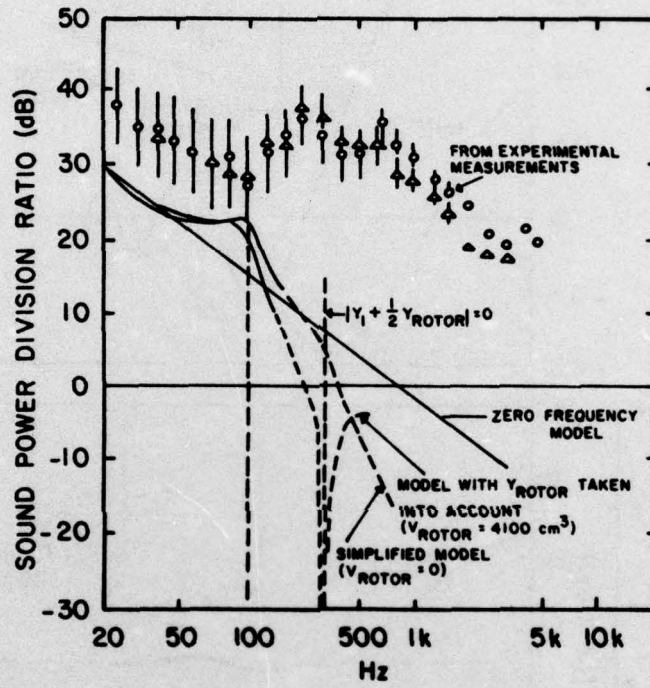
FIG. 33: SOUND POWER DIVISION RATIO (REF. 15)
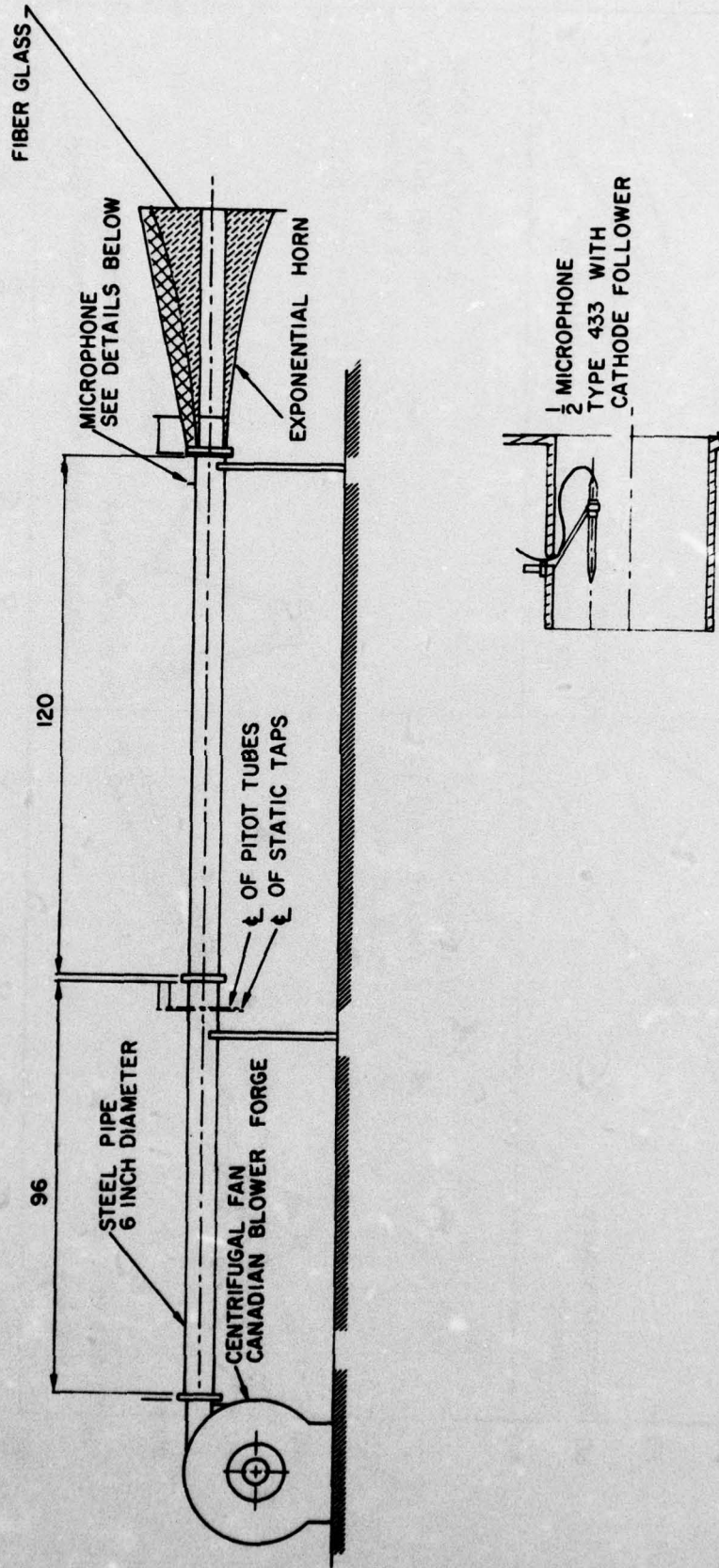
FIG. 34: EXPERIMENTAL SET-UP FOR MEASURING SOUND POWER FROM A 15 HP BLOWER
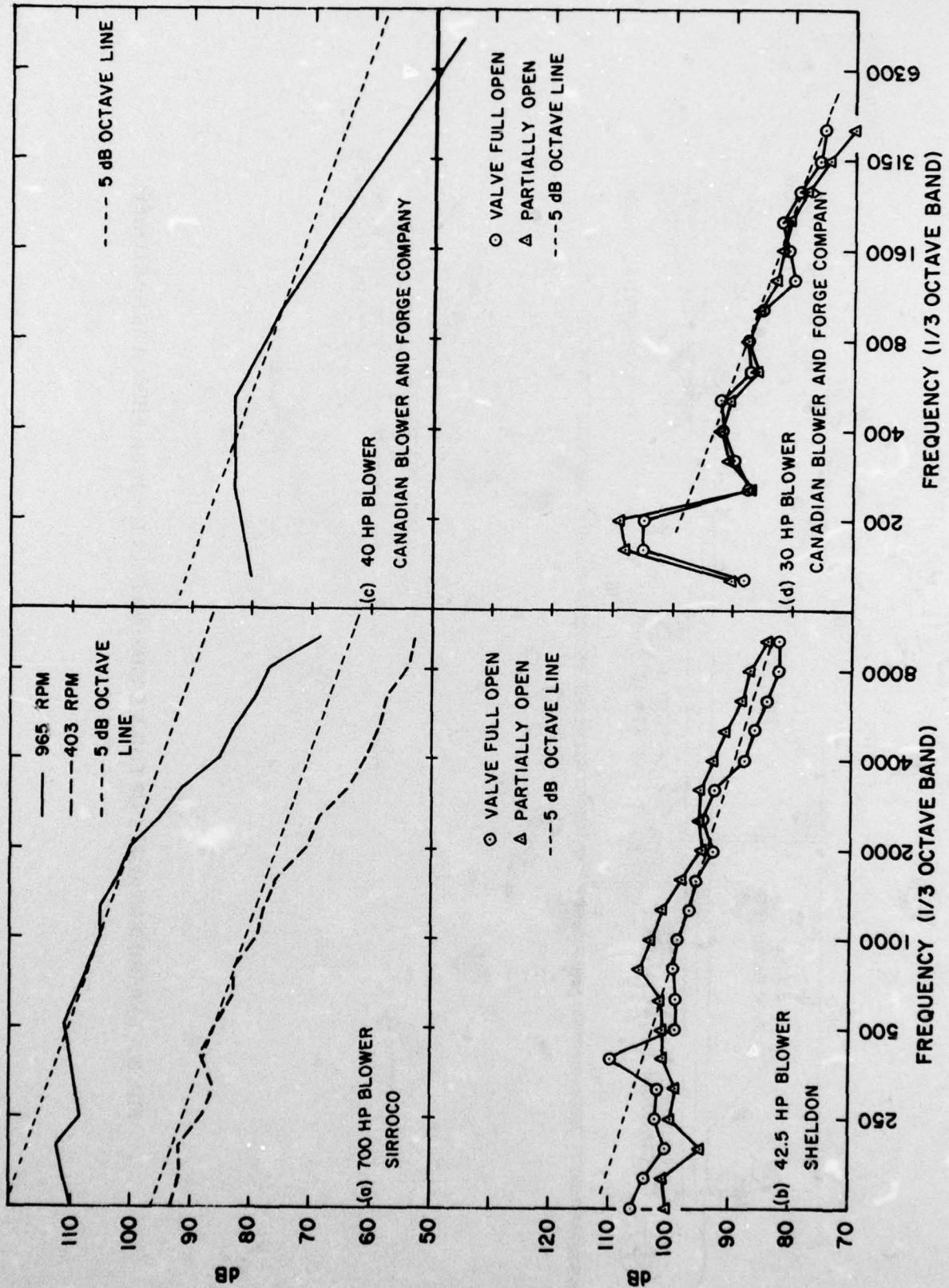
FIG. 35: NOISE SPECTRA FROM LARGE BLOWERS
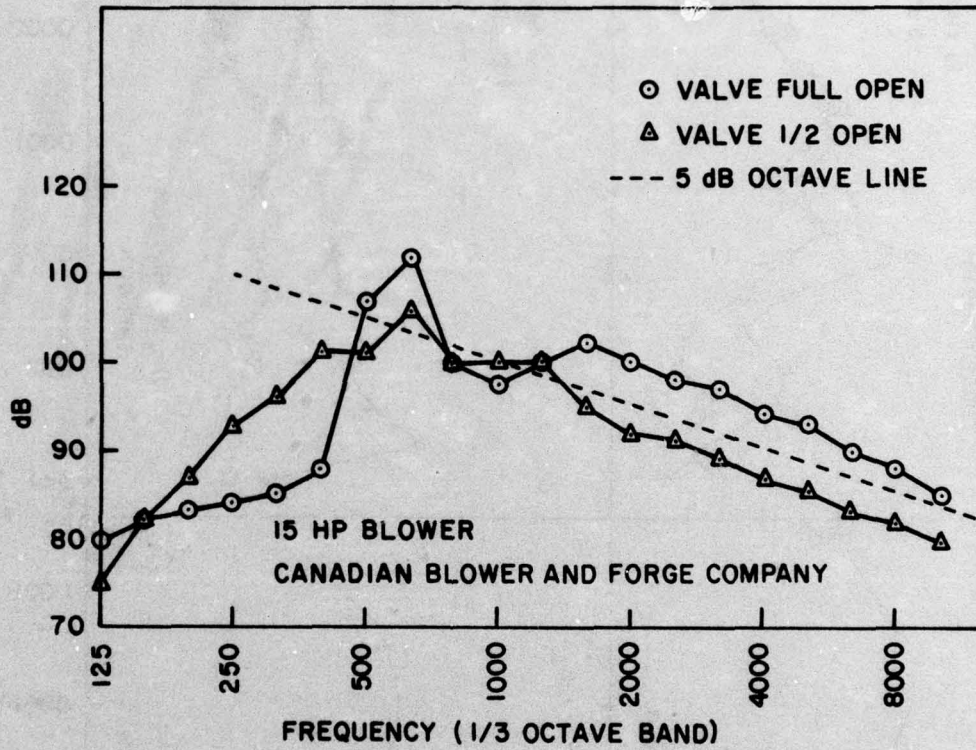
FIG. 36: NOISE SPECTRA FROM 15 HP BLOWER
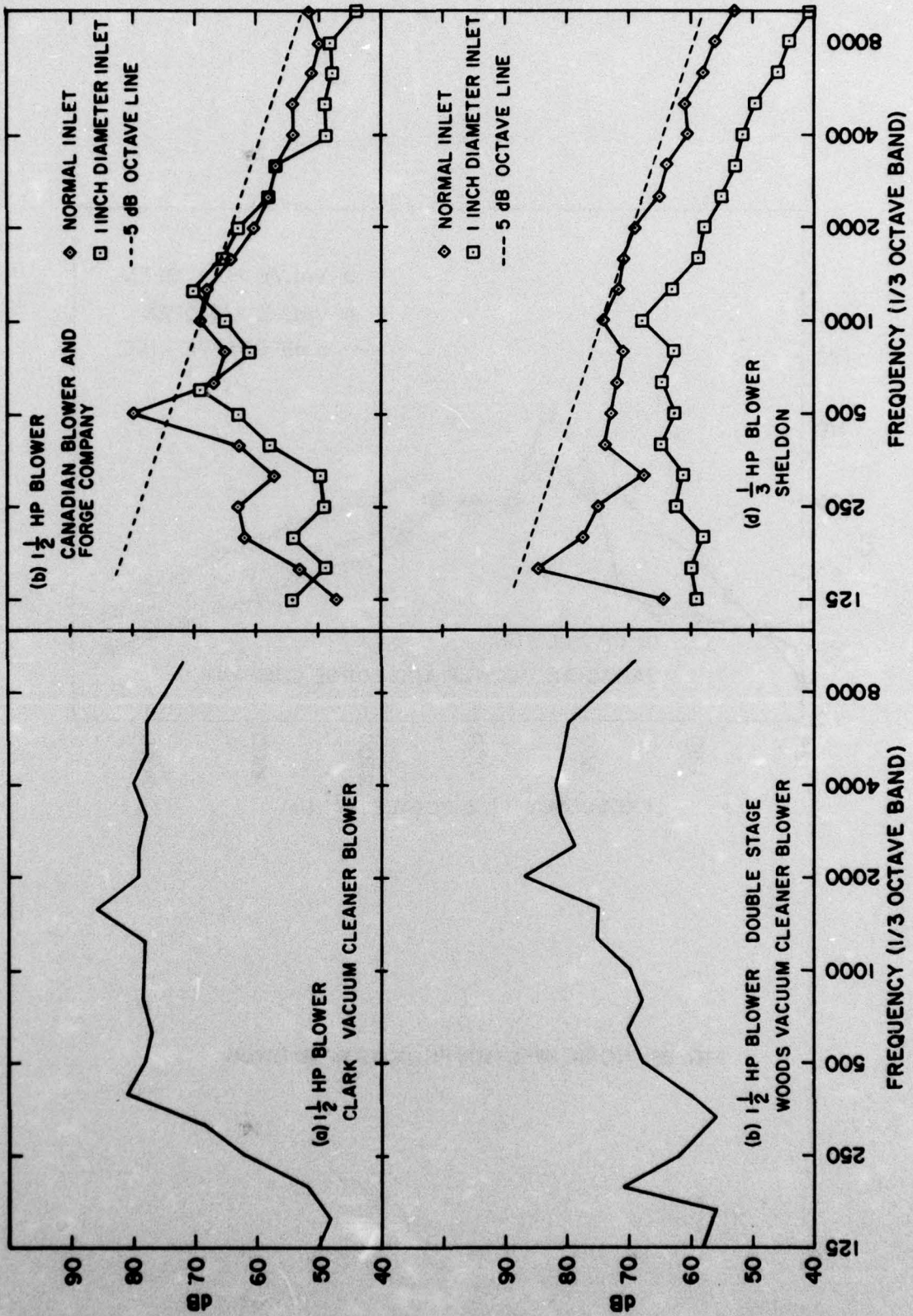
FIG. 37: NOISE SPECTRA FROM SMALL BLOWERS

NRC, DME ME-244
National Research Council Canada. Division of Mechanical Engineering.

CENTRIFUGAL BLOWER NOISE STUDIES: LITERATURE SURVEY
AND NOISE MEASUREMENTS.
Krishnappa, G. December 1976. 56 pp. (incl. figures)

A review of the existing literature on the subject of centrifugal fan
and blower noise studies is presented in this report to establish further areas
of research needed to aid in the development of a quiet blower. Noise meas-
urements on a wide variety of blowers used in the laboratory, ranging from
1/3 to 700 horsepower are described with the object of identifying important
frequency components from various types of blowers.

The existing literature suggests that the blade passing frequency
tone and its harmonics are produced by the interaction of the flow issuing
from the blade exit with the cut off edge formed by the junction of the
blower casing and its exhaust duct and that random noise is generated by the
unsteady flow processes within the impeller. The blower casing and ducted
environment are shown to exert a powerful influence on noise characteristics.
Among the various blowers tested, the prominent noise component appeared
to be the tone at the blade passing frequency.